



UNIVERSITY OF LEEDS

This is a repository copy of *Climatic versus halokinetic control on sedimentation in a dryland fluvial succession*.

White Rose Research Online URL for this paper:
<http://eprints.whiterose.ac.uk/80263/>

Version: Accepted Version

Article:

Banham, SG and Mountney, NP (2014) Climatic versus halokinetic control on sedimentation in a dryland fluvial succession. *Sedimentology*, 61 (2). 570 - 608. ISSN 0037-0746

<https://doi.org/10.1111/sed.12064>

Reuse

Unless indicated otherwise, fulltext items are protected by copyright with all rights reserved. The copyright exception in section 29 of the Copyright, Designs and Patents Act 1988 allows the making of a single copy solely for the purpose of non-commercial research or private study within the limits of fair dealing. The publisher or other rights-holder may allow further reproduction and re-use of this version - refer to the White Rose Research Online record for this item. Where records identify the publisher as the copyright holder, users can verify any specific terms of use on the publisher's website.

Takedown

If you consider content in White Rose Research Online to be in breach of UK law, please notify us by emailing eprints@whiterose.ac.uk including the URL of the record and the reason for the withdrawal request.



eprints@whiterose.ac.uk
<https://eprints.whiterose.ac.uk/>

Climatic versus halokinetic control on sedimentation in a dryland fluvial succession

Steven G. Banham¹ & Nigel P. Mountney¹

1 – Fluvial & Eolian Research Group, School of Earth and Environment, University of Leeds, Leeds, LS2 9JT, UK (E-mail: eesgb@leeds.ac.uk)

Abstract

Fluvial systems and their preserved stratigraphic expression as the fill of evolving basins are controlled by multiple factors, which can vary both spatially and temporally, including prevailing climate, sediment provenance, localised changes in the rates of creation and infill of accommodation in response to subsidence, and diversion by surface topographic features. In basins that develop in response to halokinesis, mobilised salt tends to be displaced by sediment loading to create a series of rapidly subsiding mini-basins, each separated by growing salt walls. The style and pattern of fluvial sedimentation governs the rate at which accommodation becomes filled, whereas the rate of growth of basin-bounding salt walls governs whether an emergent surface topography will develop that has the potential to divert and modify fluvial drainage pathways and thereby dictate the resultant fluvial stratigraphic architecture. Discerning the relative roles played by halokinesis and other factors such as climate-driven variations in the rate and style of sediment supply, is far from straightforward. Diverse stratigraphic architectures present in temporally equivalent, neighbouring salt-walled mini-basins demonstrate the effectiveness of topographically elevated salt walls as agents that partition and guide fluvial pathways and thereby control the loci of accumulation of fluvial successions in evolving mini-basins: drainage pathways can be focused into a single mini-basin to preserve a sand-prone fill style, whilst leaving adjoining basins relatively sand-starved. By contrast, over the evolutionary history of a suite of salt-walled mini-basins, region-wide changes in fluvial style can be shown to have been driven by changes in palaeoclimate and sediment-delivery style.

The Triassic Moenkopi Formation of the south-western USA represents the preserved expression of a dryland fluvial system that accumulated across a broad, low-relief alluvial plain, in a regressive continental to paralic setting. Within south-eastern Utah, the Moenkopi Formation accumulated in a series of actively subsiding salt-walled mini-basins, ongoing evolution of which exerted a significant control on the style of drainage and resultant pattern

of stratigraphic accumulation. Drainage pathways developed axial (parallel) to salt walls, resulting in compartmentalised accumulation of strata whereby neighbouring mini-basins record significant variations in sedimentary style at the same stratigraphic level. Despite the complexities created by halokinetic controls, the signature of climate-driven sediment delivery can be deciphered from the preserved succession by comparison with the stratigraphic expression of part of the system that accumulated beyond the influence of halokinesis, and this approach can be used to demonstrate regional variations in climate-controlled styles of sediment delivery.

Keywords: Moenkopi Formation, Salt Anticline Region, Paradox Basin, salt wall; mini-basin, fluvial, dryland, climate, halokinesis, confined flow, non-confined flow.

Introduction

Ephemeral fluvial systems that develop under the influence of arid climatic conditions are common as both present-day active alluvial systems and as successions preserved in the ancient rock record (Williams, 1971; Picard & High, 1973; Rust, 1981; Jones *et al.*, 2005; McKie *et al.*, 2010; McKie 2011). In addition to climate, basin setting, tectonic regime and rates of sediment delivery from upstream catchment areas are all important extrinsic factors that influence the style of drainage and pattern of sedimentation in ephemeral fluvial systems (Hampton & Horton, 2007; Thamo-Bozso *et al.*, 2002). As a result of the interplay between these variables, a range of different channelised and non-channelised (typically sheet-like) architectural elements – each characterised by a varied range of internal facies compositions – are recognised as the constituent geometrical bodies that comprise the accumulations of ephemeral fluvial successions (e.g. Hubert & Hyde, 1982; Nichols and Fisher, 2007; Cain & Mountney 2009, 2011). Understanding lateral and vertical arrangements of architectural elements in terms of their style of juxtaposition relative to one another is the key to building robust models with which to demonstrate the relative significance of the varied external controls that can potentially act to dictate the gross-scale architecture of such fluvial systems (Miall, 1985; Bridge and Tye, 2000; Gibling, 2006; Colombera *et al.*, 2012a, b).

The Triassic Moenkopi Formation (Olenekian to Anisian) is present across much of the south-western United States and has been interpreted to represent the

preserved accumulation of a series of genetically-related deltaic, shoreline, tidal-flat and continental alluvial and fluvial palaeoenvironments (Stuart *et al.*, 1972; Blakey & Ranney, 2008). In the southeast Utah region (Fig. 1), the Moenkopi Formation records the preserved expression of a dryland fluvial system for which the style of sedimentation was influenced to a considerable extent by long-lived and widespread arid climatic conditions that prevailed across a broad, low-relief and largely non-confined alluvial plain (Stuart *et al.*, 1972; Blakey, 1973, 1974, 1977; Dubiel, 1994). In the Salt Anticline Region (Elston, *et al.*, 1962; Cater, 1970) around the town of Moab, Utah, (Fig. 2a) the fluvial systems represented by the Moenkopi Formation were significantly influenced by syn-sedimentary halokinesis, which involved the growth of salt walls and the occasional sub-areal breaching of the surface landscape by salt diapirs (Lawton & Buck, 2006; Trudgill, 2011). Areas directly adjacent to growing salt walls experienced mini-basin subsidence (Kluth & DuChene, 2009; Rasmussen & Rasmussen, 2009; Trudgill, 2011) and the sedimentary expression of the Moenkopi Formation can be shown to have been controlled by both salt-wall growth and mini-basin subsidence (Lawton & Buck, 2006; Banham & Mountney, *in press*), resulting in a complex preserved sedimentary architectural style. By contrast, in areas outside the Salt Anticline Region – including the White Canyon region of far-south Utah (Fig 2b) – the preserved succession of the Moenkopi Formation was not influenced by subsurface halokinesis and the sedimentology was principally controlled by intrinsic fluvial processes moderated by episodic climatic trends (Mullens, 1960; Thaden *et al.*, 1964; Johnson & Thordarson, 1966; Stewart *et al.*, 1972; Blakey, 1974).

The aim of this study is to compare and contrast the processes by which the detailed facies and architectural elements preserved as deposits of a low-relief, dryland fluvial system accumulated for both a part of the system controlled dominantly by active salt tectonics (halokinesis) and a part of the system controlled by a combination of non-tectonic factors including the prevailing climatic regime, the style of sediment delivery from upstream catchment areas and intrinsic (autogenic) behaviour of the fluvial system itself. Specific objectives are as follows: (i) to interpret the processes by which lithofacies and architectural elements preserved in a low-relief, dryland fluvial system accumulated and became preserved; (ii) to describe how halokinesis in the form of salt-wall uplift and ensuing mini-basin isolation acted to control the generation and distribution of fluvial facies and architectural elements; (iii)

to develop a predictive model with which to account for spatial variations in the distribution and geometrical arrangement of architectural elements both within and away from areas of halokinetic influence; (iv) to demonstrate how variations in climate and fluvial-discharge regime influence the preserved stratigraphic architecture of dryland fluvial systems.

This work is important for the following reasons: (i) it enables development of an improved understanding of the controls that govern the formation and distribution of architectural elements in dryland fluvial systems; (ii) it enables the relative roles of external (allogenic) halokinetic and climatic controls on fluvial basin-fill architectures to be identified and examined; (iii) it provides a series of detailed depositional models with which to predict sand-body distribution in analogous settings, including economically important subsurface reservoirs such as the Triassic Skagerrak Formation (Hodgson *et al.*, 1992; Smith *et al.* 1993) of the Central North Sea, and the Pre-Caspian Basin of the Urals region (Barde *et al.*, 2002a; Newell *et al.*, 2012).

Background

Fluvial systems draining regions influenced by syn-sedimentary halokinesis and their accumulated deposits preserved in the stratigraphic record have been the focus of relatively few detailed studies at the scale whereby relationships between individual architectural elements can be determined. Early studies of fluvial successions developed in salt-walled mini-basins are those from subsurface studies of Hodgson *et al.* (1992) and Smith *et al.* (1993) regarding the economically important, hydrocarbon-bearing Triassic Joanne & Judy sandstones of the Central North Sea. McKie & Audretsch (2005); McKie & Williams (2009) and McKie (2011) undertook detailed studies of the Skagerrak Formation of the Central North Sea, specifically of the Herron Cluster (UKCS Quad 22), to determine how the preserved sedimentary architecture and drainage behaviour of a dryland fluvial succession that accumulated in a salt-withdrawal mini-basin was influenced by halokinesis. More recently, Barde *et al.* (2002a,b) and Newell *et al.* (2012) investigated the influence of halokinesis on Permo-Triassic fluvial successions in the Pre-Caspian Basin of the Urals region of Kazakhstan using a range of techniques including analysis of seismic reflection data and interpretation of satellite, wireline-log and core data to delineate depositional

environments. However, the subsurface nature of each of these studies precluded analysis of detailed relationships between architectural elements.

The Chinle Formation of the Salt Anticline Region, South East Utah, has been the subject of several studies of halokinetic influence on fluvial sedimentation (Blakey & Gubitosa 1984; Hazel, 1994; Prochnow 2006; Mathews *et al.*, 2007). Climate during accumulation of this Triassic fluvial succession is considered to have been humid, with a monsoonal component (Blakey & Ranney, 2008), and rates of sediment supply were high relative to slow rates of subsidence that arose as a consequence of the grounding of mini-basins due to complete salt withdrawal. As a consequence, fluvial architectures in the Chine Formation are characterised by high proportions of channel fill-complexes, containing coarse-grained sandstone.

Venus (2012) undertook a detailed study of the proximal part of the Cutler Group, which accumulated as an alluvial mega-fan distributive fluvial system (Barbeau, 2003; Cain & Mountney, 2009, 2011; cf. Hartley *et al.*, 2010; cf. Weismann *et al.*, 2011) succession in the Salt Anticline Region of SE Utah. This succession represents the preserved expression of a braided fluvial system for which high rates of sediment supply were sufficient to fill accommodation developed in a series of salt-walled mini-basins, thereby allowing drainage pathways to pass largely undiverted across several blind salt walls throughout much of their evolution. As drainage progressed over the crests of the salt walls, the fluvial systems apparently evolved in a manner whereby subtle changes in facies and architectural-element distributions are recorded: mean grain size systematically decreases with increasing distance from the salt walls; ponded, finer-grained elements accumulated on the upstream side of salt-walls; palaeodrainage direction in some areas was temporarily deflected from the general trend in response to episodes of salt-wall growth; aeolian elements accumulated in the sheltered lee of salt-wall generated topography. Indeed, Venus (2012) demonstrate that drainage networks of fluvial systems represented by the Cutler Group were unlikely to have been isolated in separate mini-basins due to the high rate of sediment delivery to the system that allowed drainage to occur transverse to salt wall orientation.

Basin isolation is an important factor that dictates preserved fluvial architectural expression in salt-walled mini-basins: where mini-basins are physically isolated from each other, sediment supply rates can vary significantly between adjacent basins, giving rise to the development of adjoining sand-prone and sand-

poor basins, potentially in close proximity to each other (Hodgson *et al.*, 1992; Banham & Mountney, *in press*).

Geological Setting

The Paradox Basin in which the Moenkopi Formation studied here accumulated, is a Pennsylvanian to Permian foreland basin in which more than 4000 m of strata were accumulated in the foredeep adjacent to the Uncompahgre Uplift of the Ancestral Rocky Mountains (Barbeau, 2003). During the late-stage filling of the Paradox Basin, the Uncompahgre Uplift remained an active source of clastic detritus and was a major sediment source for the Permian Cutler Group. By the early Triassic, the largely denuded uplift likely contributed only localised sources of sediment for accumulation of the Moenkopi Formation (Dubiel *et al.*, 1996; Nuccio & Condon, 1997; Banham & Mountney, *in press*), before the last remnants of the palaeo-high were buried by deposits of the Upper Triassic Chinle Formation (Blakey & Ranney, 2008; Trudgill, 2011).

The Moenkopi Formation crops out in parts of the present-day states of Arizona (Ward, 1901), New Mexico, Colorado, Utah, and Nevada (Darton, 1910; Gregory, 1917; Stewart, 1959, Carter, 1970; Blakey 1973, 1974, 1989; Hintze & Axen, 1995). This formation accumulated in a mixed fluvial, coastal plain and paralic setting, in which the shoreline underwent a gradual but prolonged marine regression throughout the Early Triassic, such that marine-influenced environments, including tidal flats, retreated to the northwest to become replaced further south by continental fluvial environments (Blakey, 1974; Blakey & Ranney, 2008). The Moenkopi Formation is divided into at least 20 formally recognised members (Blakey, 1974, 1989; Stuart *et al.*, 1972), each reflecting regional changes in depositional sub-environment.

Halokinesis initiated by differential sediment loading of the salt-bearing Pennsylvanian Paradox Formation by the Pennsylvanian-aged Honaker Trail Formation and Permian-aged Cutler Group continued from late Pennsylvanian in to the Jurassic (Doelling, 1988; Trudgill, 2011). This influenced deposition in the Salt Anticline Region of the foredeep of the Paradox Basin where accumulated salt was most thickly developed and overburden greatest (Kluth & DuChene, 2009; Rasmussen & Rasmussen, 2009; Paz *et al.*, 2009; Trudgill & Paz 2009; Venus, 2012). Salt-induced deformation extended into the Lower Triassic Moenkopi

Formation (Banham & Mountney, *in press*) and Upper Triassic Chinle Formation (Hazel 1994; Prochnow *et al.*, 2006; Matthews *et al.* 2007), as well as the Jurassic Wingate Sandstone and Kayenta Formation (Doelling, 1988; Bromley, 1989), albeit to a lesser extent than that experienced during the Permian (Fig. 1b).

The Moenkopi Formation in the Salt Anticline Region was originally described by Shoemaker and Newman (1959) and has been studied more recently by Lawton & Buck (2006) and Dodd & Clarke (2011). In the Salt Anticline Region, the formation is divided into 4 members: the Tenderfoot (lowermost), Ali-Baba, Sewemup, and Parriott (Shoemaker & Newman, 1959) (Fig. 1b). The lowermost three members are each laterally traceable both within and between a series of salt-walled mini-basins in the Richardson Amphitheater, Castle Valley, Big Bend, Moab, Potash and Shafer Basin areas (Fig. 1; Doelling & Chidsey, 2009), whereas the uppermost Parriott Member is restricted to the flanks of the Castle Valley salt wall (Shoemaker & Newman, 1959; Stuart *et al.*, 1972). The four members are delineated by distinct and mappable variations in architectural style and associated facies: the Tenderfoot Member; the Ali-Baba; the Sewemup; and the Parriott.

The Moenkopi Formation in the White Canyon region, southern Utah, is divided into 2 members: the Torrey and Hoskinnini (Blakey, 1974) (Fig 1b). The Hoskinnini Member was originally named by Baker & Reeside (1929) and was interpreted as part of the Cutler Group, before being re-interpreted as a basal member of the Moenkopi Formation (Stuart, 1959). This unit was later re-interpreted again as a separate formation by Blakey (1974), who considered it to have accumulated in a separate isolated basin, therefore representing a transitional unit between the Permian and Triassic successions. The Hoskinnini Member shares many similar characteristics with that of the Tenderfoot Member observed in the Salt-Anticline Region (especially in the Fisher basin), and has previously been considered a lateral equivalent (Stuart, 1959). The Torrey Member (referred to as the lower slope-forming, cliff-forming and upper ledge-forming members by Stuart *et al.*, 1972) was considered in detail in this study, with basic observations being made for the Hoskinnini Member. The depositional limit of the Sinbad Limestone, Black Dragon and Moody Canyon Members each pinch out near Hite Crossing beyond the limit of this study (Blakey, 1974; O'Sullivan & MacLachlan, 1975).

The palaeoclimate of the Moenkopi Formation has long been considered to have been arid (Stuart *et al.*, 1972; Blakey, 1974; Morales, 1987; Stokes 1987;

Blakey & Ranney, 2008), with the palaeoenvironment having formed an extremely low-relief, low-gradient alluvial plain, based on analysis of mineral composition and textural maturity of the accumulated sandstone and the sheet-like preserved architectural expression of fluvial elements (Blakey, 1974).

Data and Methods

For this study, 49 vertical profiles were measured: 38 from the Salt Anticline Region and 11 from the White Canyon area. To complement these data, drawn architectural panels and photomontages depicting the distribution and style of juxtaposition of architectural elements and lithofacies were used to generate a series of correlation panels and architectural element models. Stratigraphic surfaces of significant lateral extent and which bound major architectural elements were traced between measured profiles to aid correlation; oblique aerial photography was used to assist tracing of key stratal surfaces where outcrop was inaccessible or difficult to observe from on the ground.

Of the 38 measured vertical profiles from the Salt Anticline Region, which collectively record >9000 m of stratigraphic succession, 22 measured sections record continuous profiles through the entire thickness of the Moenkopi Formation from the basal contact with the underlying Cutler Group or White Rim Sandstone (a capping formation of the Cutler Group), to the unconformable base of the overlying Chinle Formation (Fig. 1b). The total preserved thickness of the Moenkopi Formation varies from 125 m to 245 m, with significant variations both within and between salt-walled mini-basins. The majority of the remaining measured sections from the Salt Anticline Region record either the basal or top unconformities that bound the formation. For all measured sections, the stratigraphic position of the bases of the various members can be identified with confidence.

Each of the 11 measured vertical profiles from the White Canyon study area record the full thickness of the Torrey Member of the Moenkopi Formation, from the contact with the underlying Hoskinnini Member (as defined by Blakey, 1974), through to the unconformity that defines the contact with the overlying Chinle Formation (Fig. 1b). The preserved thickness of Moenkopi Formation varies from 60 to 110 m.

Palaeocurrent analysis was undertaken in all of the mini-basins observed within the Salt Anticline Region and White Canyon Region to determine the drainage direction and potential regions of sediment supply. Statistics including the vector mean and vector magnitude were calculated using methods described by Lindholm (1987). In total, 233 indicators of palaeoflow were measured from sedimentary structures including ripple-crests, climbing-ripple strata, cross bedding foreset azimuths and channel axes.

Sedimentology and Stratigraphy

Lithofacies

Fifteen distinct and commonly occurring lithofacies types are identified throughout the study areas (Salt Anticline Region, SAR; White Canyon Region, WCR) (Table 1; Fig. 3), with the majority of lithofacies being demonstrably of fluvial origin; the remainder are a product of evaporitic or aeolian processes, though examples of such types occur as accumulations of only local extent and limited thickness. Representative vertical profiles for both the Salt Anticline Region (Fig. 4a) and White Canyon Region (Fig. 4b) demonstrate the typical stratigraphic styles preserved in the study areas. Vertical profiles for the Salt Anticline Region (Fig. 4a) portray representative parts of the succession for each of three separate mini basins studied: the Fisher, Parriott and Big Bend basins (Fig 2a). The profiles demonstrate variations in preserved fluvial expression between neighbouring mini-basins. Vertical profiles for the White Canyon area (Fig 4b) portray representative parts of the succession across the southern-most study area.

Architectural Elements

Representative examples of fluvial architectures present in both study areas depict common architectural elements in the Salt Anticline Region and White Canyon Region (Fig. 5). Fluvial facies are grouped into 2 facies associations corresponding to (i) channelised deposition and (ii) non-confined, sheet-like deposition. Four distinct architectural elements (F1 to F4) are associated with channelised deposition; five other distinct architectural elements (F5 to F9) are associated with non-confined deposition. Each architectural element is composed internally of lithofacies assemblages that typically occur as predictable vertical or lateral successions, and

each element type exhibits distinctive geometric properties (Fig. 6) and styles of juxtaposition to neighbouring elements.

Multi-storey, multi-lateral channel-fill elements (F1)

Description: F1 elements (Fig. 5a,e,f,g) are typically 3 to 10 m thick and comprise laterally and vertically amalgamated packages of strata. A representative vertical succession through an F1 element consists of a series one or more 0.2 to 2 m-thick cosets. Each coset is defined at its base by a 5th-order erosional bounding surface (Fig. 5a; Miall, 1996), commonly with a pebble-lag of either intra- or extra-formational clasts (typically no more than 0.3 m thick but rarely up to 0.6 m thick) lying directly upon it. The lowermost basal unit in each coset is succeeded upwards by multiple stacked sets of trough- or high-angle-inclined planar cross-bedding (Fxt/ha Fxp), the two forms being difficult to differentiate in cases where the outcrop trend is parallel to the original bedform migration direction. Cross-bedded sandstone sets rarely pass gradationally upward into sets of climbing-ripple-stratified sandstone (Frc/Fxl) or homogeneous siltstone (Fhiss), but in most cases, such successions are not fully preserved because the base of the overlying coset erodes into upper part of the underlying one. Individual storeys represented by cosets of strata can be traced laterally for 50 to 300 m; their erosional basal surfaces exhibit up to 0.5 m of relief and they are typically cut-out laterally by adjacent storeys. Groups of laterally or vertically amalgamated storeys collectively characterise a single F1 element, examples of which can be traced in directions perpendicular and parallel to regional palaeoflow for up to 2 km and 10 km, respectively. Although relief due to incision is present at the base of F1 elements in the form of a 6th order bounding surfaces of significant lateral extent (Miall, 1996), it rarely exceeds 1 m.

Interpretation: Multi-storey multi-lateral channel-fill elements represent the deposits of laterally extensive, aggrading braid-belts (Fig. 7a; cf. Flores & Pillmore, 1987; Gibling, 2006). These elements are the preserved expression of sandy macro-forms that migrated axially within channels, which themselves formed part of a wider active braided channel complex (cf. Miall, 1996; McKie 2011). The occurrence of gravel lags in association with erosively based channel storeys indicates high-energy flow where stream power was sufficiently high to result in incision into the underlying substrate, followed by localised transport of pebble-grade material (mostly mud-chip rip-up

clasts) prior to deposition as a basal lag, probably in the immediate aftermath of peak-flood discharge on the falling limb of the hydrograph (cf. McKie, 2011). A combination of rapid downstream and lateral barform migration and expansion, frequent localised channel avulsion and high rates of sediment delivery over a protracted period generated multiple laterally amalgamated and vertically stacked storeys (cf. Cain & Mountney 2009); the erosional surfaces that bound each storey could have arisen either through lateral channel migration, barform migration or barform expansion within a broad channel (cf. Picard & High, 1973; Miall, 1996; Bridge, 2003). The repeated stacking of multiple storeys resulted in the generation of a laterally extensive sheet-like body of composite channel-fill elements to form the F1 element. Internally, although erosional bounding surfaces that define storeys are numerous, few such surfaces define distinct channel margins. These multi-storey multi-lateral elements were preserved through a combination of lateral avulsion of channels, possible lateral migration of the entire channel belt and by the aggradation of the system to allow the vertical accumulation and stacking of later storeys of channel-fills (Gibling, 2006). The considerable overprinting of vertically-stacked storeys could indicate a relatively low rate of generation of accommodation space or might alternatively indicate a high frequency of avulsion (Bristow & Best, 1993). The multi-storey and multi-lateral nature of these composite channel-fill elements indicates a significant and possibly long-lived episode of fluvial activity in a localised area to allow the accumulation of these stacked sheet-like bodies (Cain & Mountney, 2009).

Single-storey, multi-lateral channel-fill elements (F2)

Description: F2 elements are composed internally of laterally but not vertically amalgamated channel-fill storeys that are each 0.5 to 2 m thick (Fig. 5b). The basal surfaces of these elements are sharp and many exhibit incision (up to 1 m of relief, though typically no more than a few decimetres). Vertical facies successions in these elements are encapsulated within a single coset of cross strata that forms a storey, though storeys are stacked laterally adjacent to each other, with their bounding surfaces typically showing local lateral incision into neighbouring storeys. Cosets representing storeys are delineated by a basal erosion surface that commonly has pebble (and rarely cobble) intraformational clasts (Fci) associated with it. These lags are overlain by sets of trough or high-angle-inclined planar cross-bedded strata

(Fxt/ha Fxp). Rarely, sets of low-angle-inclined sandstone (la Fxp) are observed but these never comprise more than a few percent of the element. Cross-bedded sets present in F2 elements are typically overlain by F5 elements (sheet-like heterolithic bodies) containing sets of climbing-ripple strata (Frc/Fxl), overlain by horizontally interbedded sandstone and siltstone (Fhiss). These elements are typically laterally extensive and many can be traced for over 2 km in orientations perpendicular to regional palaeoflow.

Interpretation: Single-storey, multi-lateral channel-fill elements represent non-aggrading laterally extensive and laterally mobile braid-belts which were succeeded by non-confined sheet-like elements (Fig. 7b). These elements are dominated by bedload transport processes, with cross-bedded sets representing the downstream migration of dune-scale mesoforms (Miall 1996). The only rare presence of low-angle-inclined Fxt lithofacies indicates that these elements did not migrate laterally to any significant degree; rather, sedimentation occurred predominantly as a result of down-channel migration of sandy bedforms (Miall, 1996). The laterally extensive “sheet-like” nature of these amalgamated channel complexes arose from repeated avulsion of active channels at a single stratigraphic horizon to form a channel belt (Martinsen *et al.*, 1999; Gibling 2006). Original channel width is difficult to determine from outcrop study, but is likely to have been several hundred metres to possibly in excess of 1 km (cf. Tunbridge 1981). The style of termination of F2 elements, which are overlain by non-channelised elements of various types, indicates that the braid-belt either avulsed abruptly to an alternative location elsewhere on the alluvial plain (cf. Mackey & Bridge, 1995; Bridge 2003), else a cessation of channelised fluvial activity occurred throughout the region in favour of non-confined sedimentation, possibly in response to a change to a more arid climate (Blum & Tornqvist, 2000) or to a shut-down in sediment delivery (Leeder *et al.*, 1998).

Single-storey unilateral (isolated) channel-fill elements with abundant infraformational clasts (F3)

Description: Isolated F3 channel elements typically occur embedded within F1 and F2 elements, although they also occur as isolated forms encased in non-confined elements. F3 elements are discernable from F1 & F2 elements by virtue of their distinctive fill of pebble-grade clasts of intraformational origin. F3 elements are

typically defined by steep-sided channel margins inclined up to 50°, channel fills are 0.5 to 1.5 m thick and up to 15 m wide. F3 elements are overlain either by non-confined elements or are partly eroded by channelised elements. Clasts are angular, composed of argillaceous siltstone and (more rarely) mudstone that was apparently derived from the local vicinity, and have diameters from 10 mm to 0.4 m. The style of fill of these F3 elements by intraformational clasts may give rise to either a massive (structureless) fabric (Fci) or result in the preservation of crude cross-bedding (Fxt with Fci). The matrix present between the clasts is fine-grained sand.

Interpretation: Isolated, intraformational clast-filled elements represent the preserved product of erosion and reworking of argillaceous material derived locally from the surrounding alluvial plain and the subsequent deposition of this material in thread-like channels, probably in a single cut-and-fill event related to an individual flood (Fig. 7a; Billi, 2007; Cain & Mountney, 2009). A possible variation on this mechanism for the generation of these elements could have arisen where locally active fluvial systems encroached onto the flanks of a pre-existing topographic high, resulting in localised erosion, entrainment, transport and deposition through incision (c.f. [Rodríguez-López et al., 2012](#)) and collapse at the outer bank of the channel (Gomez-Gras & Alonso-Zarza, 2002). In places, F3 elements can be shown to be associated with locations proximal to topographic features on the alluvial plain, including topography generated by salt-wall uplift (discussed later).

Massive (structureless) & horizontally laminated channel elements (F4)

Description: F4 elements are typically up to 8 m thick, and are characterised at their base by a 1 to 2 m-thick set of massive bedded sandstone (Fm), overlain by a 6 to 7 m-thick set of horizontally bedded sandstone (Fh), bedding surfaces of which reveal primary current lineation. Basal incision typically exhibits modest relief that rarely exceeds 1 to 2 m. These elements typically occur adjacent to multi-storey (F1), and single storey (F2) multi-lateral channel-fill elements and in close proximity to the flanks of salt walls, notably in the vicinity of the Castle Valley salt wall in the Parriott basin.

Interpretation: Massive (structureless) and horizontally laminated sandstone channel-fill elements (Fig. 6) most likely represent rapid incision and subsequent fill during a

single flood event. The basal part of the channel-fill association represents rapid deposition from suspension, before flow velocities waned and upper plane-bed conditions prevailed (Ashley *et al.*, 1990). The presence of a single facies succession, most of which was horizontally laminated sandstone (Fh) with primary current lineation demonstrates accumulation from a fast-moving flow arising from a single flood event (McKee *et al.*, 1966).

Sheet-like heterolithic elements (F5)

Description: Elements composed of heterolithic strata are laterally extensive and can be typically be traced laterally over many square kilometres; they comprise >75% of the total vertical succession in some areas. A typical vertical facies succession within this element may include a basal massive-bedded (Fm) sandstone sheet, which may have a coarse-grained sand lag and erosive relief of up to a few tens of millimetres. Massive sandstone (where present) is overlain by sets of climbing-ripple strata (Frc/Fxl), within which ripple trains usually climb at a subcritical angle (Fig 6). These pass gradationally upward into sets of homogenous or laminated siltstone (Fhiss) at the top of the succession. Single examples of these sheet-like elements are typically only 0.1 to 0.4 m thick, but can occur in repeating cycles that are collectively >20 m thick (Figs. 5d,e). Sheet-like elements can occur juxtaposed laterally with channelised elements (F1 to F4) (Fig. 5g), or vertically (Figs 5a,b,e,f), where successive channelised elements have incised into the pre-existing sheet-like heterolithic elements.

Interpretation: These heterolithic sheet-like elements are the preserved expression of repeated non-confined flood events that distributed thin sheets of sediment across the alluvial plain during episodes of elevated discharge (Fig. 7d). Each element, defined by a fining-upward cycle, likely represents an individual flood event, where a predictable facies succession is deposited, corresponding to deposition from a waning flow. The lowermost massive sandstone sets, which typically possess a low-relief and a sharp erosional base, represent the passage of an initial flood bore, which possessed sufficient energy to entrain sediment from underlying flood deposits before depositing them either through progressive accretion or via rapid suspension settling as the flood-front passed (Blair, 2000). The facies succession in the upper part of the element is characteristic of a progressive reduction of flow competence,

with the relatively thick accumulations of bed-load generated structures such as climbing-ripple strata being diagnostic (Benvenuti *et al.*, 2005; Hampton & Horton, 2007). Water depth of the sheet-like flood waters was likely between 0.07 and 0.8 m (Rahn, 1967; Bentham *et al.*, 1993; Tooth, 1999a; Blair, 2000), although water depth may have increased where chute elements (F8) occur. Radial spreading of water over a considerable area (cf. Fisher *et al.*, 2008) and transmission losses would have resulted in dissipation of the flood water and eventual deposition of lower-stage plane beds and the settling of argillaceous siltstone from suspension during the final phase of the flood when flow velocity decreased to approach zero (Hampton & Horton, 2007). Repeated, stacked cycles of these elements demonstrate that sheet-flood events were a dominant process in parts of the Moenkopi Formation.

Gypsum-clast-bearing elements (F6)

Description: Gypsum-clast-bearing elements are restricted to the Sewemup Member and are characterised by 0.1 to 0.4 m-thick accumulations that can either be clast-supported (FGc) or matrix-supported (FGm), with a fine sand matrix. Such clast-rich sets can typically be traced laterally for several hundred metres. Clasts are composed predominantly of detrital gypsum, although intra-formational clasts of reworked argillaceous silt and fine sand and extremely rare extra-formational clasts are also typically present. Gypsum-clast-bearing sets are typically overlain by sets of climbing-ripple strata (Frc/Fxl), which are capped by a siltstone set (Fhiss) (Fig. 6). These gypsum clast elements are only observed within 5 to 8 kilometres of the Castle Valley salt wall.

Interpretation: Gypsum clast horizons represent the preserved expression of fluvial erosion and entrainment of diaper-derived gypsum detritus (Figs 7e; Lawton & Buck, 2006). During episodes where salt-wall uplift exceeded the rate of sedimentation, actively uplifting salt walls breached the land surface, forming salt glaciers (cf. Ala, 1974; Talbot & Rogers, 1980) which acted as an episodic source of detritus that was subsequently reworked by fluvial activity (Banham & Mountney, *in press*). These clasts were transported up to several km from the flank of the salt wall by flood waters before being deposited as clast-bearing units. The proportion of clasts-to-matrix in such units is a function of transport distance from the salt wall and gypsum availability (itself a function of the ratio of salt-wall uplift and sedimentation rate).

Partly confined over-spill element (F7)

Description: These elements, which are typically several 100 metres wide, are characterised by a sheet-like geometry and occur in close association with chute elements (F8), typically embedded within them in areas adjacent to channel-fill complexes (F1 & F2) (Fig. 6). Characteristic vertical facies successions of these elements comprise coarse-grained, horizontally-laminated sandstone (Fh), within which F8 chute elements may be embedded, overlain by typically climbing-ripple strata (Frc) and interbedded very-fine sand and silt (Fhiss). These sheet-like successions are each typically 0.5 to 2 m thick and may occur vertically stacked as repeating cycles of fining-upward facies successions. These elements typically occur nested within a succession composed of other sheet-like elements, including sheet-like heterolithic and pond elements (F5 and F9). Significantly, these elements typically only occur in close proximity (within 500 m) of uplifted salt walls.

Interpretation: Partly confined over-spill elements represent the deposits of non-channelised flows that originated as splays from channels during flood episodes when bank-full capacity was exceeded and flow spread across the floodplain in an unconfined manner (Fig. 7f). Rather than radially dissipating across the floodplain as for conventional non-confined flows, an elevated feature, such as salt-wall-generated topography, acted to partially confine the flow. Such partial confinement resulted in water depth and velocity locally increasing, enabling the flow to erode and transport relatively coarse-grained sediment across the floodplain before depositing this load either as chute elements in locations where floodwaters converged to form a small channelised feature (F8) filled with crudely cross-bedded deposits, or as a coarse-grained, horizontally laminated sandstone in a non-confined setting (F7). As flood waters subsided and flow velocity waned, the falling-stage sedimentary succession (typically climbing-ripple strata) accumulated, followed by suspension settling of very-fine sand and silt (Tunbridge 1981b; Miall 1985).

Chute elements with coarse-grained fill (F8)

Description: These elements occur as 0.1 to 0.4 m thick, medium-grained sandstone to granulestone lenses, with erosive relief of up to 0.1 m on their basal surface. These elements can typically be traced laterally for up to 20 m before they pass abruptly into sheet-like heterolithic elements (F5). The fill of these chute elements is

either of massive sandstone (Fm), or crude trough cross-bedding (Fxt), and is normally overlain by a heterolithic sheet-element succession of climbing-ripple laminated strata (Frc/Fxl) and siltstone (Fhiss).

Interpretation: Chute elements represent the preserved expression of the convergence of non-confined floodwater on the floodplain to form minor channels (Fig 7d; Abdullatif, 1989; Field, 2001; Benvenuti, 2005; Cain & Mountney 2009, 2011). The localised convergence of flood waters induced local deepening and increased flow velocity (cf. Field, 2001), which encouraged incision and the local entrainment and transport of coarser-grained sediment via bed-load transport, possibly with the winnowing of finer-grained material (Hjulstrom, 1935; Sundborg 1956). Rapid deposition of coarse-grained material from suspension resulted in the accumulation of structureless sandstone, whereas gradual waning of the late-stage flow induced deposition from bed-load transport and the formation of crude cross-bedding (Fxt). These chute elements likely carried flow for no more than a few hundred metres before passing back into a non-confined flow (cf. Cain & Mountney, 2011).

Floodplain pond elements (F9)

Description: Pond elements are characterised internally by associations of wave-rippled sandstones (WR) and homogeneous or horizontally laminated siltstone, with fine-grained deposits commonly possessing well developed and distinctive desiccation cracks that are up to 0.6 m deep and filled with structureless siltstone or fine sandstone. Sandstone in these elements is commonly reduced to a grey colour. Individual pond elements are 0.2 to 0.5 m thick, and can typically be traced for 10 to 40 m laterally, though the largest example has been traced over an area of 25,000 m².

Interpretation: Pond elements record sedimentation in the aftermath of flood events. Floodwaters accumulated in very shallow depressions on the floodplain and formed shallow ponds of standing water, which may have persisted for several days or weeks (cf. Picard & High, 1973; Fisher *et al.*, 2008). Wind blowing over the surface of these ponds generated surface waves, which in turn allowed symmetrical ripple-forms to develop on the fine-grained sandy substrate (Allen, 1968). Silt settled from suspension. Loess transported by aeolian processes in the arid environment was

likely trapped to form an additional sediment component. Evaporation and infiltration of water caused the surface to dry out and resulted in the generation of desiccation cracks, with larger cracks indicative of slower rates of desiccation.

Spatial & Temporal Variations in Sedimentary Architecture

This study considers the Moenkopi Formation in two distinct geographical areas, each with their own tectonic and provenance history. The Moenkopi Formation in the Salt Anticline Region was influenced by ongoing salt tectonics throughout the period of deposition (Rasmussen & Rasmussen, 2009; Kluth & DuChene, 2009; Trudgill & Paz, 2009; Trudgill, 2011). As a result of this halokinetic influence, the Moenkopi Formation accumulated in a series of isolated salt-walled mini-basins, each with a unique sediment supply and subsidence regime (Banham & Mountney, *in press*). The effects of this isolation resulted in the preservation of significantly different styles of fluvial architecture. By contrast, the Moenkopi Formation in the White Canyon area lacks evidence for a tectonic control but instead records a strong climatic signature that is additionally modified by the impact of spatial variations in accumulation style that arose as a result of autogenic fluvial processes.

Salt Anticline Region

Within the Salt Anticline Region, the Moenkopi Formation accumulated in three distinct mini-basins (Fig. 2a): the Fisher basin between the Uncompahgre Front and the Fisher Valley salt wall, the Parriott Basin between the Fisher Valley and Castle Valley salt walls, and the Big Bend Basin (Banham & Mountney, *in press*) between the Castle Valley and Moab (Lisbon) Valley salt wall. The preserved thickness of the Moenkopi Formation varies between the studied mini-basins, as a function of both the subsidence history of individual basin segments and location within individual mini-basins (e.g. depocentre versus flank); the thickest preserved succession (245 m) occurs in the Big Bend Basin.

The Moenkopi Formation in the Salt Anticline Region is separated from the underlying Permian Cutler Group by an angular unconformity that accounts for approximately 25 Ma of non-deposition and erosion (Rasmussen and Rasmussen, 2009), with the angular nature of the unconformity having developed in response to continued and progressive salt movement between the cessation of Cutler Group sedimentation and the onset of Moenkopi Formation sedimentation (Trudgill, 2011).

Although the sedimentary character of the four members of the Moenkopi Formation tends to vary between each studied mini-basin (Fig. 9), the preserved fluvial successions in each mini-basin share a common association of lithofacies and architectural-element types (Figs 6 and 7a/b). Throughout accumulation of the Moenkopi Formation, the fluvial system drained from southeast to northwest, parallel to the trend of the linear salt walls (Fig. 9).

Tenderfoot Member

The basal Tenderfoot Member attains a maximum thickness of 70 m at the Fisher Valley Head locality in the Fisher basin (Fig. 10) but thins to only 40 m at the Mile 25 locality in Richardson Amphitheater. In the Parriott Basin, the maximum recorded thickness is 40 m at Castle Tower and the member is generally slope forming. The basal-most part of this member is characterised by fluvial strata with embedded clasts apparently derived from localised reworking of the uppermost strata of the underlying Cutler Group. A prominent feature of this member is a 1 to 2.5 m-thick gypsum bed (GC) that is laterally continuous throughout the Parriott Basin (Fig. 10), and which is also present in the north-eastern part of the Big Bend Basin, though has apparently been largely eroded along the southern margin of the Fisher Basin. This gypsum bed is characterised by a saccharoidal, crystalline texture that has been interpreted previously to have accumulated either in a restricted tidal-flat (sabkha) setting within a large embayment (Stuart *et al.*, 1972; Baldwin, 1973) or as an aeolianite (Lawton & Buck, 2006).

Although poorly exposed in the Parriott and Big-Bend basins, the beds overlying the gypsum horizon, which are locally composed of coarse-grained sandstone with distinctive angular grains and a gypsum cement, weather to a distinctive orange colour making them a useful marker unit. In the Fisher Basin, the Tenderfoot Member forms distinct cliffs, which are brown-orange in colour and beds have a predominantly rounded profile. As a result, the beds are better exposed and can be characterised by distinctive wavy or crinkly-laminated sandstones (facies Scls), considered to be indicative of repeated salt precipitation and dissolution in a sabkha-like environment (Goodall *et al.*, 2000). Fluvial-channel elements are generally absent. Conical-shaped de-watering structures (Fig. 5A) similar to those observed in the Hoskinnini Member (Stuart, 1959; Chan, 1989; Dubiel *et al.*, 1996) occur at one locality in the transfer zone between the Cache Valley salt wall and the

Fisher Valley salt wall (Fig.2: 3 km northwest of Log 16). These features are typically 1 to 2 m in height and occur as “megapolygons” (Chan 1989; Dubiel 1996) that are traceable over an area of 100 m² but are apparently confined both spatially and temporally to this single area in the Salt Anticline Region, with no other examples observed in this study area.

Ali Baba Member

The cliff-forming Ali Baba Member has a sedimentary character that differs significantly between the Fisher and Parriott basins (Fig. 10). In the Fisher Basin, the member is ~50 m thick, and is characterised by medium- to coarse-grained sandstone with localised pebble lags and rare beds of pebble-grade orthoconglomerate (Fce). Metre-thick sets of tabular and trough cross-bedding (Fxp/Fxt) are common. In the Parriott Basin the member is 25 to 40 m thick and is characterised by interbedded siltstone and fine- to medium-grained sandstone (Fhiss) in both the basal- and upper-most parts. By contrast, the middle part of the member is characterised by a prominent 8 to 10 m-thick cliff-forming sandstone composite bedset composed of dual-storey, multilateral channel-fill elements (F1) and massive & horizontally laminated channel-fill elements (F4), which are well exposed along the flanks of the Castle Valley and along the side of Parriott Mesa and the Priest and Nuns mesas. This prominent, laterally extensive bedset is largely massively bedded (Fm) in the Castle Tower area, but exhibits trough (Fxt) and planar-tabular (Fxp) cross-bedding near Adobe Mesa and the Priest & Nuns mesas. Associated lithofacies present in this member include, ripple forms (both current and wave ripples) and ripple cross-lamination (Frc & WR), structureless sandstone beds (Fm), primary current lineation (Fh), lags of mud-chip rip-up clasts of intraformational origin (Fci), plus bedding surfaces preserving obstacle scours and desiccation cracks.

Fluvial architectural elements in the Ali-Baba Member are dominantly characterised by 1 to 2 m-thick single-storey multi-lateral channel-elements (F2) in the Parriott and Big Bend basins, but are additionally characterised by 6 to 10 m-thick, vertically-stacked and amalgamated multi-storey channel elements (F1) in the Fisher Basin, and up to 8 m thick massive & horizontally laminated channel-fill elements (F4) in the Parriott Basin. Larger multi-storey channel-element complexes can be traced laterally for distances in excess of 10 km in orientations parallel to palaeoflow (i.e. in orientations parallel to the strike of the linear salt walls). Heterolithic units of

interbedded siltstones and sandstones in the Parriott Basin form sheet-like fluvial elements (F3) that are each laterally continuous for at least 200 m, with some examples extending for in excess of 1 km.

Sewemup Member

The sedimentary character of the Sewemup Member varies between each studied mini-basin, but the member as a whole is slope forming (Fig. 10). The maximum preserved thickness is 110 m at Castle Tower and elsewhere along the southwest side of the Parriott Basin. The member thins to the northeast toward the Onion Creek–Fisher Valley salt wall in the Parriott Basin.

One diagnostic feature of the Sewemup Member adjacent to the Castle Valley salt wall is the widespread occurrence of several distinctive gypsum-clast-bearing beds (Fig 3) (clasts 10 to 200 mm diameter; mean 100 mm), each up to 1 m thick (FGc/m). These beds tend to be orthoconglomerates (FGc) in areas within 2000 m of the Castle Valley salt wall but are paraconglomerates (FGm) in areas toward the centre of the mini-basins. Gypsum clasts are absent from the Fisher Basin and from parts of the Parriott Basin adjacent to the Onion Creek-Fisher Valley salt wall. Common sedimentary structures in the Sewemup Member include desiccation cracks, small gutter channels (0.1 m-deep) (F8), a range of dewatering structures including load casts and flame structures, overturned, and convolute bedding (Fd).

Common architectural elements of the Sewemup Member include laterally extensive bodies with sheet-like geometries that are composed internally of heterolithic siltstone and sandstone beds (Fhiss, F6) and which are traceable for distances in excess of 1000 metres. Single-storey channel-fill elements (F2) are rare and, where present, they are relatively small (0.3 to 1 m thick; mean 0.4 m), with width:thickness ratios that range from 25:1 to over 250:1, and with fills that are characterised by trough cross-bedding (Fxt) and massive (structureless) fine-grained sandstone (Fm). High-angle-inclined fractures (10-30 mm wide) filled with fibrous gypsum and typically arranged in an anastomosing pattern are a distinctive non-sedimentary feature of this member.

Parriott Member

The Parriott Member attains a maximum thickness of 40 m adjacent to the Castle Valley salt wall and thins toward the Onion Creek – Fisher Valley salt wall, pinching out over the crest of this salt wall. Typically, the member is 15 to 30 m thick but is

mostly absent over the crests of the salt walls, either due to non-deposition on the highs created by salt-wall uplift, or uplift and erosion prior to the onset of the accumulation of the overlying Chinle Formation. An exception to this is a 10 m-thick succession preserved on the nose of the Castle Valley salt wall (in the Red Hills area; Fig. 10).

The Parriott Member is characterised by an absence of gypsum clasts (FGc/m), with the succession containing a high proportion of multi-storey channel-fill elements (F1) around the flanks of the Castle Valley salt wall, and single-storey channel-fill (F2) & heterolithic sheet-like elements (F5) elsewhere in the basins. The central and north-eastern parts of the Parriott Basin are characterised by rare and isolated occurrences of single-storey multi-lateral channel elements (F2), each 1 to 2 m thick and several hundred metres wide. Adjacent to the nose of the Castle Valley salt-wall in the Parriott Basin (at the so called Truck-and-Boat structure; Fig. 10) a dual-storey fluvial channel-fill element (F1) forms a distinctive feature, which is laterally continuous for 950 m before it is cut-out by recent erosion. In the Big Bend Basin adjacent to the Castle Valley salt wall, the Parriott Member is characterised by multi-lateral and multi-storey channel elements (F1) that collectively form a major fluvial-channel complex that extends laterally for in excess of 1000 m.

The boundary between the Moenkopi Formation and the overlying Chinle Formation is marked by a disconformity across much of the Salt Anticline Region, although locally this boundary is represented by a distinctive angular unconformity in areas immediately adjacent to the salt-walls, indicating uplift of the salt-walls during or after the latter stages of deposition of the Moenkopi Formation but prior to the onset of accumulation of the Chinle Formation.

Palaeocurrent data and sediment provenance

Analyses of palaeocurrent data from the orientations of ripple crests and lee-slope azimuths in climbing-ripple strata, trough and high-angle planar cross-bedded sandstone in the Salt Anticline Region indicate dominant palaeo-drainage that was consistently toward the northwest throughout accumulation of the Moenkopi Formation (Fig. 1b) (vector mean = 302°, vector magnitude = 0.86; n = 177). Data from individual mini-basins also reflect this overall trend (Fisher Basin: vector mean = 305°, vector magnitude = 0.91; n = 88. Parriott Basin: vector mean = 303°, vector magnitude = 0.85; n = 57. Big Bend Basin: vector mean = 292°, vector magnitude =

0.77; $n = 32$). Crests of wave ripples on exposed bedding surfaces created by bi-oscillating currents in bodies of standing water (F9: pond elements) throughout the Salt Anticline Region have a vector mean trend of 052° (vector magnitude = 0.73; $n = 62$), a trend that suggests a NW- or SE-oriented prevailing palaeowind (Fig 1b).

Provenance and petrographic analyses (Stuart *et al.*, 1972) suggest a dominant sediment source for the Moenkopi Formation in the Salt Anticline Region from the San Luis Uplift. However, the abundance of extraformational conglomerates of Uncompahgre affinity in the Ali-Baba Member in the Fisher Basin indicates a dual source of sediment during the initial phase of accumulation in this mini-basin. The confinement of this secondary source of extraformational clasts solely to the Fisher Basin suggests that salt-wall-generated surface topography acted to prevent the transverse delivery of sediment from the Uncompahgre Uplift into the Parriott or Big Bend basins (Banham & Mountney, *in press*). The Tenderfoot Member contains an abundance of reworked sediment, which has been interpreted as a reworked remnant of the White Rim Sandstone (Dubiel *et al.*, 1996).

White Canyon Region

The White Canyon study area in southeast Utah extends from Copper Point in the north to Moss Back Butte in the southeast, and across to Whirlwind Draw in the Clay Hills region to the southwest of the study area (Fig. 2). The only member of the Moenkopi Formation studied in this area is the Torrey Member (Blakey, 1974). In the southern part of the study area, the Moenkopi Formation lies apparently conformably on top of the Hoskinnini Member (Fig 11 & 12, the boundary being differentiated by a change in colour and bedding style: the Hoskinnini is generally a deeper orange colour, is thicker-bedded, has a rounded weathering profile and exhibits undulatory bedding; Stewart, 1959; Dubiel, 1992). The outcrop expression of the Hoskinnini Member shares many characteristics observed in the Tenderfoot Member of the Salt Anticline Region, including crenulated wavy laminations (Fig. 12; Stuart, 1959). Where the Hoskinnini Member is absent, the Moenkopi Formation lies disconformably on the Permian Organ Rock Formation (Cain & Mountney, 2009). The Moenkopi Formation throughout this study area is disconformably overlain by the Chinle Formation, which is differentiated from the Moenkopi Formation by a marked increase in grain-size (from very-fine sand and silt to very-coarse sand and pebbles where the basal Shinramup conglomerate is present). Incision of up to 8 m into the

underlying Moenkopi Formation by channelised elements of the overlying Chinle Formation is indicated by the presence of distinctive yellow, purple or grey mottling in the basal 10 m of the Chinle Formation and, in some localities, an abundance of petrified wood.

Hoskinnini Member

The Hoskinnini Member, where observed, is typically 30 m thick and forms distinct, orange-coloured cliffs at the base of the Moenkopi Formation (Fig. 12). The beds forming these cliffs have a rounded profile, and some exhibit large-scale deformation manifest as low amplitude undulating beds (Fig. 12; “Crinkly beds” – Stuart, 1959). In addition, enigmatic conical-shaped fluid-escape structures similar to those observed in the Tenderfoot Member of the Salt Anticline Region have been documented in the region (Stuart, 1959; Chan 1989; Dubiel, 1992; Dubiel *et al.*, 1996). In the Clay Hills area, a 1 to 2 m thick crystalline gypsum bed is present, which exhibits similar characteristics to the gypsum bed of the Tenderfoot Member of the Salt Anticline Region.

Torrey Member

Within the study area, the Torrey Member varies from 90 m thick in the southwest, to 64 m thick in the north, to only 45 m thick in the southeast, with an overall south-westerly thinning due to progressive erosion at the top of the succession. The member is characterised by a stepped profile that was originally divided into Lower slope-forming, ledge-forming, and upper slope-forming members (Stewart *et al.*, 1972) that correspond generally to slope-forming sheet-like heterolithic elements (F5) and cliff-forming channel fill-complex elements (F1, F2). Spatial variations in sand content are discernable, with a higher proportion of channel elements in the upper third of the member in the vicinity of Steer Gulch, Happy Jack Mine and Copper Point logs (Figs 2b, 4b). A distinctive set of 4 or 5 beds containing intraformational-clasts out crop in the lower 10 to 30 m of the member, and these are typically interbedded with thin siltstone beds (Fig. 5b). These useful markers were observed in 8 of the 11 studied sections, spread over an area of 20 by 40 km. Within the overlying 10 to 20 m of the succession, beds disrupted by soft-sediment deformation (Fd) are common, with the deformation style indicative of structures arising due to upward escape of water, including load and flame structures and sand volcanoes, that occur in close proximity to sand lobes and slump structures (cf. Owen, 1987, 1996).

Channelised fluvial architectural elements (F1, F2) can, in nearly all cases, be traced laterally for in excess of 500 m and in some instances for 10 km. Sheet-like heterolithic elements (F5) are highly laterally extensive and can be traced for tens of km in directions both parallel and perpendicular to palaeoflow. Silt-prone sheet-like elements (F5) are particularly prevalent in the upper portion of the succession in the west of the study area, where they account for over 75% of the interval. Gypsum-clast-bearing elements (F6) are rare and are only observed in the south-western part of the study area. A single example of gypsum clasts preserved within trough cross-bedded strata was observed in the Clay Hills region. The origin of these gypsum clasts is uncertain, but may relate to the gypsum bed present in the Hoskinnini Member.

Palaeocurrent data and sediment provenance

Palaeocurrent direction in the Torrey Member throughout the White Canyon study area has a vector mean of 333° with a magnitude of 0.89 (n = 56). This favours a likely provenance from the Defiance Upwarp (Figs. 1 & 11), to the southwest of the study area (Stuart *et al.*, 1972, Fillmore, 2011), a region composed of Permian strata, including the distal fringes of the Organ Rock Formation, the undifferentiated Cutler Group, and the De Chelley Sandstone (Stewart *et al.*, 1972; Stanesco *et al.*, 2000).

Discussion

Combined facies and architectural-element analysis demonstrates significant complexity in terms of spatial and temporal variations in the deposits of the Monekopi Formation. Although a similar set of lithofacies is present in both study areas, which are indicative of the operation of broadly similar sedimentary processes, significant local variations in the spatial (lateral) and temporal (vertical) arrangement of architectural elements composed of these facies are recognised. Such variations are here shown to have arisen in response to the impact of different sets of allogenic controls including: (i) tectonic (halokinetic) regime, which dictated the rate of generation of accommodation space, the width of basin floor over which the fluvial systems could spread and the location of the salt walls; (ii) climatic regime, which was unlikely to have been significantly different between the two study areas but which may have varied temporally; (iii) the rate and pathway of sediment delivery from both the principal and secondary source areas, which themselves are controlled

by salt-wall location. Additionally, local variations in sedimentary character likely also reflect the various autogenic processes that operated in the fluvial systems, including avulsion style and frequency and the mechanisms by which bank-full channel capacity was exceeded during floods to result in sheet-like, non-confined overland flow.

Environment of deposition

Architectural element analysis demonstrates that accumulation of sediment was dominated by relatively thin but laterally extensive bodies: most F1 and F2 channel elements have width-to-thickness ratios greater than 250:1; sheet-like elements (F5, F6) have width-to-thickness ratios greater than 2000:1. These thin but laterally extensive elements demonstrate a broad, low-relief accumulation surface. Architectural elements with distinctive assemblages of lithofacies (Table 1) in both channelised and non-channelised elements indicate sedimentation via repeated, low-frequency, high-magnitude ephemeral flood events (Williams, 1970, 1971; Glennie, 1970; Picard & High, 1973; Gee, 1990). Individual sedimentary components characteristic of an arid environment are as follows: desiccation cracks (up to 0.6m deep) indicative of slow episodes of desiccation in non-confined elements (F6, F7, F8); gypsum-clast-bearing elements (F6), rare tee-pee structures; the presence of a crystalline gypsum unit, which demonstrates that the region of deposition endured episodes of sustained aridity to allow preservation of such soluble material. Facies associations of laterally extensive sheet-like elements (F5), including thin, massively bedded sandstones (Fm), climbing-ripple strata (Frc/Fxl) and homogeneous and horizontally laminated siltstone (Fhiss) demonstrate evidence for rapid deposition from a waning flow (Williams 1971). Thin pond elements (F9) mostly of limited lateral extent and with fills of wind-generated wave-ripple strata (Allen, 1968) demonstrate the presence of shallow pools of standing water; the near-ubiquitous presence of desiccation cracks indicates complete desiccation of the pools; in some examples, the presence of desiccation cracks at multiple closely spaced stratigraphic levels demonstrates repeated flooding and desiccation, and the transient nature of the ponds.

Non-confined flows in extra-channel settings are widely documented as a product of episodic, high-energy ephemeral floods in arid alluvial environments (e.g. Rahn, 1967; Glennie, 1970; Williams, 1970, 1971; Tooth, 1999a/b, 2000). Such flows,

which are typified by markedly peaked hydrographs (Reid *et al.*, 1998), are generally capable of transporting and distributing large volumes of sediment over relatively short periods (Frostick *et al.*, 1983).

Although channel elements are relatively abundant in the preserved stratigraphy, at any given time channelised forms likely only occupied a small proportion of the surface area, as is common in many ephemeral alluvial systems (just 3% in the examples studied by Rust & Legun, 1983), thereby implying that most sediment transport and deposition occurred as a result of non-confined fluvial processes. It is the increased preservation potential of erosively-based channel elements and their overprinting of non-confined elements (e.g. via lateral accretion and avulsion processes) that results in them comprising a larger proportion of the *preserved* stratigraphic succession.

Hampton & Horton (2007) recognised sheetflow deposits by virtue of their thin and laterally extensive nature, with poorly defined channel banks with low clay content (cf. North *et al.*, 2007) characterised by high width-to-depth ratios. Such poorly defined, high aspect ratio channel elements (>300:1) may be extremely difficult to discern in parts of the succession dominated by non-confined elements, especially if they are in-filled by heterolithic facies associations.

A general depositional model depicting the relationship between confined and non-confined architectural elements observed in the Moenkopi Formation and their likely mode of generation is shown in Fig. 8. Channel belts consisting of multiple, shallow and potentially poorly defined braided channel networks (cf. North, 2007; Hampton & Horton, 2007) soon exceeded bank-full capacity during rising flood stage, resulting in over-spill of flood waters onto the adjoining alluvial plain. Non-confined flood waters transported and distributed sediment as both bed load and suspended load across a low-relief alluvial plain. As flood waters emanated away from the confined channel networks, the flood-front dissipated radially across the alluvial plain. Transmission losses due to a combination of infiltration and evaporation increased as the flood waters became spread over a larger area, resulting in a progressive reduction in both flow velocity and stream power (Bull, 1979), thereby leading to the sequential accumulation of the succession of facies representative of waning flow characteristic of non-confined elements (F5) and the preservation of pond elements (F9). Occasionally, these non-confined flood waters converged locally, resulting in

the formation of minor chute elements (F8), which run for a few tens to hundreds of metres before flooding out and dissipating (cf. Field, 2001; Cain & Mountney, 2009).

Halokinetic control on sediment accumulation

The style of sedimentary architecture in both the Salt Anticline Region and the White Canyon area is similar: both are characterised by shared facies associations and several similar architectural elements. However, significant differences in the proportions of facies and the arrangement of elements are recognised. Most significantly, the formation is significantly thicker in the mini-basins of the Salt Anticline Region (typically twice as thick).

A number of elements are unique to the Salt Anticline Region: unilateral intraformational clast-filled channel elements (F3); salt-wall-derived gypsum-clast-bearing elements (F6; Lawton & Buck, 2006); partly confined over-spill elements (F7). These elements require the presence of salt-wall generated topography to form, either by acting as a source of clastic material (intraformational clasts or gypsum detritus) or by acting to confine flow and modify fluvial activity.

The main influence of halokinesis on the accumulating succession is recorded by the distribution of fluvial elements within the studied mini-basins, whereby basin isolation induced by salt-wall uplift controlled architectural-element distribution between mini-basins (Banham & Mountney, *in press*).

Figure 9 depicts a general depositional model to account for the style accumulation of fluvial elements in areas adjoining uplifting salt walls, whereby the distribution of elements varies between neighbouring mini-basins. The model depicts how the Fisher Valley salt wall isolated the Fisher and Parriott mini-basins, thereby acting as a control on the resultant style of accumulation. The Fisher Basin, which received clastic input from both the Uncompahgre and San Luis Uplifts during the accumulation of the Ali Baba Member, represents a sand-prone interval, where high rates of sand delivery coupled with low rates of subsidence allowed the formation of braid-belts which resulted in the accumulation of single-storey channel-fill complexes (F2) that subsequently amalgamated vertically to form multi-storey channel-fill complexes (F1). Additionally, partly confined over-spill elements (F7) are prevalent in the Fisher Basin, where they onlap onto the uplifted salt wall flank (Fig 10).

The Parriott Basin received clastic input solely from the San-Luis uplift, which resulted in accumulation of a sand-poor interval during the accumulation of the Ali

Baba Member: fluvial activity in this basin was diminished relative to that of the neighbouring Fisher Basin, resulting in accumulation of a higher proportion of argillaceous elements (Fhiss). The absence of major channel networks in this basin precluded significant reworking of this argillaceous material.

Climatic Control on sediment accumulation

Evidence for climatic variation in the Moenkopi Formation is recorded as subtle upward (vertical) changes in the overall style of sedimentation that can be discerned and correlated across both study regions. In the Salt Anticline Region, climatic signatures are masked by the preserved effects of other controls, including varying rates of mini-basin subsidence and sediment supply. However, the overall style of sedimentary architecture changes through the Moenkopi Formation (Fig. 10) and this is likely to have occurred as a function of palaeoclimate.

Throughout accumulation of the Tenderfoot, (and the laterally equivalent Hoskinnini Member – Stewart, 1959) conditions were interpreted to be arid and deposition occurred in a sabkha-like setting (Dubiel, 1994), resulting in accumulation of lithofacies Scls in the Fisher Basin, with few channel-fill complexes preserved. The Ali Baba Member in the Salt Anticline Region is characterised by multi-storey channel-fill complexes (F1) in the Fisher Basin, by single-storey channel-fill complexes (F2) with sheet-like heterolithic strata (F5) in the Parriott Basin, and by a mixture of sheet-like heterolithic elements (F5) and rare single-storey channel-fill elements (F2) in the Big Bend Basin. Collectively, this indicates a region-wide increase in humidity relative to the underlying member, resulting in an increased sediment influx into the mini-basins and an increase in channelised fluvial activity (Rumsby & Macklin, 1994). The Sewemup Member in all of the studied basins is characterised by an abundance of sheet-like heterolithic strata (F5) and gypsum-clast-bearing elements (F6), with few single-storey channel-fill complexes (F2). These elements demonstrate a decrease in fluvial activity across all three mini-basins at this stratigraphic level and record an episode when major flood events did not occur. The fluvial reworking and subsequent preservation of highly-soluble gypsum clasts demonstrates the ephemeral nature of the fluvial system and the overall arid climate. During accumulation of the Parriott Member, a higher proportion of single-storey (mainly in the Parriott Basin) and multi-storey channel-fill elements

(F2, F1) were preserved, demonstrating a return to relatively less arid climatic conditions.

Climatic signatures recorded in the Moenkopi Formation of the White Canyon area are less obvious, in part due to the preservation of a thinner succession. However, a channel-prone interval in the middle part of the Torrey Member (the so-called Ledge-Forming Member of Stewart *et al.*, 1972) tentatively correlates with the Ali Baba Member of the Salt Anticline Region based on similar sedimentary character. This would suggest that both study regions shared a common climatic regime, resulting in coeval variations in sediment supply and similar stratigraphic expressions.

Conclusions

The Moenkopi Formation in the Salt Anticline Region and White Canyon area of southern Utah is the preserved expression of a partly channelised and partly non-channelised fluvial succession that accumulated across a low-relief alluvial plain (Fig 13). The prevailing palaeoclimate at the time of accumulation was arid, as reflected in the style of the preserved strata. Depositional style is characterised by accumulation of vertically amalgamated, laterally extensive sheet-like bodies throughout most parts of the formation. These sheet-like bodies are either (i) channel-belt complexes that lacked significant basal erosional relief, composed of single- and multi-storey, multi-lateral channel-fill complexes, or (ii) sheet-like elements with heterolithic internal fills that are the preserved expression of non-confined fluvial flow across an extensive alluvial plain.

Both the Salt Anticline Region and White Canyon area share common facies and architectural elements, indicating the action of comparable fluvial processes under similar climatic conditions across the region. The rate of sediment accumulation in the Salt Anticline Region was controlled primarily by rate of accommodation generation via differential rates of mini-basin subsidence, with sediment supply rate and pathways having governed the accumulation of sand-prone and sand-poor styles of basin fill in neighbouring mini-basins. The absence of halokinetic processes controlling the distribution of fluvial elements in the White Canyon Region allowed autocyclic processes (lateral channel migration & avulsion) to act as dominant controls on fluvial element distribution in this region. Although halokinesis did not exert a primary control on fluvial sedimentary architecture, as demonstrated by the presence of common facies and architectural elements in both

study areas, salt-wall uplift did however result in the generation of certain unique facies, element types and relationships, including unilateral channel elements with intraclast fills (F3), gypsum-clast-bearing elements, originating from salt glaciers where salt walls breached the land surface (F6), and partially-confined over-spill elements (F7). The direction of sediment delivery, the presence of a single or multiple areas of sediment provenance, and the rate of sediment supply all played important roles in the development of basin-fill style, with higher overall rates of sediment supply favouring the development of sand-prone basins containing high proportions of channel-fill elements and lower rates of sedimentation favouring the development of sand-poor basins, characterised by elements deposited by non-confined flow. Climatic variations are discerned from changes in sediment supply rate and subsidence rate manifest as coeval variations in the overall style of accumulation, including, for example, the shift in the styles of sedimentation discernable between the Ali Baba Member and the Sewemup Member. By contrast, localised changes in sediment supply rate or basin subsidence rate typically only result in a change in the style of accumulation in a single mini-basin.

The Moenkopi Formation records how the signature of spatial and temporal variations in sediment supply rate, orientation and pathway of sediment delivery, rates of halokinesis, and climate change are manifest in the preserved stratigraphic succession of a dryland fluvial system. The predictable distribution of fluvial elements accumulated in a series of salt-walled mini-basins can be used to develop models to account for the distribution of fluvial elements in subsurface hydrocarbon plays, such as the Central North Sea, or Pre-Caspian Basin of Kazakhstan.

Acknowledgements

This research was supported by funding from Areva, BHP Billiton, ConocoPhillips, Nexen, Saudi Aramco, Shell and Woodside through their sponsorship of the Fluvial & Eolian Research Group at the University of Leeds. Layla Cartwright is thanked for field assistance. Jo Venus, Tom Randles, Russell Dubiel, Tom Dodd, Stuart Clarke and Bill McCaffrey provided valuable field discussions. Reviewers Juan Pedro Rodriguez-López and Timothy F. Lawton, Associate Editor Mariano Marzo, and Chief Editor Stephen Rice are thanked for their constructive comments and advice.

References

- Abdullatif, O.M.** (1989) Channel-fill and sheet-flood facies sequences in the ephemeral terminal River Gash, Kassala, Sudan. *Sed. Geol.* **63**, 171-184.
- Ala, M.A.** (1974) Salt Diapirism in Southern Iran. *Am. Assoc. Petrol. Geol. Bull.*, **58**, 1758-1770.
- Allen, J.R.L.** (1968) Current Ripples: Their relation to patterns of water and sediment motion. *North-Holland Publishing Company, Amsterdam.*
- Ashley G.M. (Chair Person) and Others** (1990) Classification of Large-Scale Subaqueous bedforms: A new look at an old problem. *J. Sed Petrology*, **60**, 160-172.
- Baker, A.A. and Reeside, J.B.** (1929) Correlation of the Permian of southern Utah, northern Arizona, northwest New Mexico, and southwestern Colorado. *Am. Assoc. Petrol. Geol. Bull.*, **13**, 1413-1448.
- Baldwin, E.J.** (1983) The Moenkopi Formation of North-Central Arizona: and Interpretation of Ancient Environments based upon Sedimentary Structures and Stratification types. *J. Sed. Petrol.* **43**, 92-106.
- Banham, S.G. and Mountney, N.P.** (2013) Controls on fluvial sedimentary architecture and sediment fill state in salt-walled mini-basins: Triassic Moenkopi Formation, Salt Anticline Region, SE Utah, USA. *Basin Res.* DOI: 10.1111/bre.12022
- Barbeau, D.L.** (2003) A flexural model for the Paradox Basin: implications for the tectonics of the Ancestral Rocky Mountains. *Basin Res*, **15**, 97-115.
- Barde, J-P., Garalla, P., Harwijanto, J., and Marsky, J.,** (2002a). Exploration at the eastern edge of the Precaspian basin: Impact of data integration on Upper Permian and Triassic prospectivity. *Am. Assoc. Petrol. Geol. Bull.*, **86**, 399-415.
- Barde, J-P., Chamberlain, P., Galavazi, M., Gralla, P., Harwijanto, J., Marsky, J., and Van Den Belt, F.** (2002b). Sedimentation during halokinesis: Permo-Triassic reservoirs of the Saigak Field, Precaspian Basin, Kazakhstan. *Petrol. Geosci.*, **8**, 177-187.
- Bentham, P.A. Talling, P.J., and Burbank, D.W.** (1993) Braided stream and flood-plain deposition in a rapidly aggrading basin: the Escanilla formation, Spanish Pyrenees. In: *Braided Rivers* (Eds. J.L. Best, C.S. Bristow), *Geol. Soc. London Spec. Publ.* **75**, 177-194.
- Benvenuti, M., Carnicelli, S., Ferarri, G. and Sagri M.** (2005) Depositional processes in latest Pleistocene and Holocene ephemeral streams of the Main Ethiopian Rift (Ethiopia). In: *Fluvial Sedimentology VII* (Eds M.D. Blum, S.B. Marriott, S.F. Leclair) *IAS Spec. Publ.*, **35**, 277-294.
- Billi, P.** (2007) Morphology and sediment dynamics of ephemeral stream terminal distributary systems in the Kobo Basin (northern Welo, Ethiopia). *Geomorphology*, **85**, 98-113.

- Blair, T.C.** (2000) Sedimentology and progressive tectonic unconformities of the sheetflood-dominated Hell's Gate alluvial fan, Death Valley, California. *Sed. Geol.*, **132**, 233-262.
- Blakey, R.C.** (1973) Stratigraphy and Origin of the Moenkopi Formation (Triassic) of Southeastern Utah. *The Mountain Geologist*, **10**, 1-17.
- Blakey, R.C.** (1974) Stratigraphy and Depositional Analysis of the Moenkopi Formation Southeastern Utah. *Utah geological and Mineral Survey, Utah department of Natural Resources*, **104**.
- Blakey, R.C.** (1989) Triassic and Jurassic Geology of the southern Colorado Plateau. In: *J.P. Jenny, S.J. Reynolds, Geological evolution of Arizona, Tuscon, Arizona Geological Society Digest*. **17**, 369-396.
- Blakey, R.C. and Gubitosa, R.** (1984) Controls on sandstone body geometry and architecture in the Chinle Formation (Upper Triassic) Colorado Plateau. *Sed. Geol.*, **38**, 51-86.
- Blakey R.C. and Ranney W.** (2008) Ancient Landscapes of the Colorado Plateau. *Grand Canyon Association, Grand Canyon, Arizona*.
- Blum, M.D. and Tornqvist T.E.** (2000) Fluvial responses to climate and sea-level change: a review and look forward. *Sedimentology*, **47**, 2-48.
- Bridge, J.S.** (2003) Rivers and Floodplains: forms, processes and sedimentary record. *Blackwell Science, Oxford*.
- Bridge, J.S. and Tye, R.S.** (2000) Interpreting the Dimentions of Ancient Fluvial Channel Bars, Channels, and Channel Belts from Wireline-Logs and Cores. *Am. Assoc. Petrol. Geol. Bull.*, **84**, 1205-1228.
- Bristow, C.S., and Best, J.L.** (1993) Braided rivers: perspectives and problems. In: *Braded Rivers (Eds J.L. Best, C.S. Bristow)*. *Spec. Publ. Geol. Soc. London*, **75**, 1-11.
- Bromley, M.H.** (1991). Architectural features of the Kayenta Formation (Lower Jurassic), Colorado Plateau, USA: relationship to salt tectonics in the Paradox Basin. *Sediment. Geol.*, **73**. 77-99.
- Bull, W.B.** (1979) Threshold of critical power in streams. *Geol. Soc Am. Bull*, **90**, 453-464.
- Cain, S.A.** (2009) Sedimentology and stratigraphy of a terminal fluvial fan system: the Permian Organ Rock Formation, South East Utah. *PhD Thesis, Keele University*.
- Cain, S.A. and Mountney, N.P.** (2009) Spatial and temporal evolution of a terminal fluvial fan system: the Permian Organ Rock Formation, South-east Utah, USA. *Sedimentology*, **56**, 1774-1800.

Carter, F.W. (1970) Geology of the Salt Anticline Region in Southwestern Colorado. Department of the Interior, United States Geological Survey Bulletin, **637**.

Chan M.A. (1989) Erg margin of the Permian White Rim Sandstone, SE Utah. *Sedimentology*, **36**, 235-251.

Colombera, L., Felletti, F., Mountney, N.P. and McCaffrey, W.D. (2012) A database approach for constraining stochastic simulations of the sedimentary heterogeneity of fluvial reservoirs. *Am. Assoc. Petrol. Geol. Bull.* **96**, 2143-2166.

Colombera, L., Mountney, N.P., and McCaffrey, W.D. (2012) A relational database for the digitization of fluvial architecture: concepts and example applications. *Petrol. Geosci.* **18**, 129-140.

Darton, N.H. (1910) A reconnaissance of parts of northwestern New Mexico and northern Arizona. Department of the Interior, United States Geological Survey Bulletin, **435**.

Dodd, T.J.H and Clarke, S.M (2011) Salt Controls on Sedimentation in a Marginal-Marine to Continental Setting: Implications for Facies Development and Hydrocarbon Entrapment. *Unpublished M.Sc. Thesis*, Keele University.

Doelling, H.H. (1988) Geology of the Salt Valley Anticline and Arches National Park. Grand County , Utah. In: *Salt Deformation in the Paradox Region* (Eds H.H. Doelling, C.G. Oviatt, P.W. Huntoon), *Utah Geol. Surv. Bull.*, **122**, 7-58.

Doelling, H.H and Chidsey, T.C. (2009) Deadhorse State Park and Vicinity Geologic Road Logs, Utah. In: *The Paradox Basin Revisited: New Developments in Petroleum Systems and Basin Analysis* (Eds W.S. Houston, L.L. Wray and P.G. Moreland). *Rocky Mountain Association of Geologists Spec. Publ.*, 635-672.

Dubiel, R.F., Stanesco, J.D. and Huntoon, J.E. (1992) Clastic Sabkha Facies and Paleogroundwater Flow in the Hoskinnini Member of the Moenkopi Formation (Triassic Paradox Basin) – Implications for Hydrocarbon Emplacement. *SEPM – Rocky Mountain Section Newsletter*, **12**, 2.

Dubiel, R. F. (1994). Triassic deposystems, paleogeography, and paleoclimate of the Western Interior. *Mesozoic systems of the Rocky Mountain region, USA*, Rocky Mountain SEPM, 133-168.

Dubiel, R.F., Huntoon, J.E., Stanesco, J.D., Condon, S.M. and Mickelson, D. (1996) Permian-Triassic Depositional Systems, Paleogeography, Paleoclimate, and Hydrocarbon Resources in Canyonlands, Utah. Colorado Geological Survey, Open-File Report 96-4, Field Trip 5.

Elston, D.P. and Shoemaker, E.M. (1962) Uncompahgre front and salt anticline region of the Paradox Basin, Colorado and Utah. *Am. Assoc. Petrol. Geol. Bull.*, **46**, 1857-1878.

- Field, J.** (2001) Channel avulsion on alluvial fans in southern Arizona. *Geomorphology*, **37**, 93-104.
- Fillmore, R.** (2011) *Geological evolution of the Colorado Plateau of Eastern Utah and Western Colorado*. University of Utah Press.
- Fisher, J.A., Krapf, C.B.E., Lang, S.C., Nichols, G.J. and Payenberg, T.H.D.** (2008) Sedimentology and architecture of the Douglas Creek terminal splay, Lake Eyre, central Australia. *Sedimentology*, **55**, 1915-1930.
- Flores, R.M. and Pillmore, C.L.** (1987) Tectonic Control on Alluvial Paleoarchitecture and of the Cretaceous and Tertiary Ration Basin, Colorado and New Mexico. In: *Recent Developments in Fluvial Sedimentology, Spec. Publ. SEPM*, **39**.
- Frostick, L.E., Reid, I. and Layman, J.T.** (1983) Changing size distribution of suspended sediment in arid-zone flash floods. *Spec Publ. Int. Ass. Sediment.* **6**, 97-106.
- Gee D.M., Anderson, M.G. and Baird, L.** (1990) Large-Scale Floodplain Modelling. *Earth Surf. Process. Landf.*, **15**, 513-523.
- Gibling, M.R.** (2006) Width and Thickness of fluvial channel bodies and valley fills in the geological record: A literature compilation and classification. *J. Sed. Res.*, **76**, 731-770.
- Glennie, K.W.** (1970) Desert Sedimentary Environments. *Developments in Sedimentology 14*, Elsevier Publishing Company, Amsterdam.
- Goodall, T.M., North, C.P. and Glennie, K.W.** (2000) Surface and subsurface sedimentary structures produced by salt crusts. *Sedimentology*, **47**, 99-118.
- Gregory, H.E.** (1917) Geology of the Navajo Country: A reconnaissance of parts of Arizona, New Mexico, and Utah. Department of the Interior, United States Geological Survey Professional Paper **93**.
- Gomez-Gras, D., and Alonso-Zarza, A.M.** (2003) Reworked calcretes: their significance in the reconstruction of alluvial sequences (Permian and Triassic, Minorca Balearic Islands, Spain) *Sed. Geol.*, **158**, 299-319.
- Hampton, B.A., and Horton B.K.** (2007) Sheetflow fluvial processes in a rapidly subsiding basin, Altiplano plateau Bolivia. *Sedimentology*, **54**, 1121-1147.
- Hartley, A.J., Weissmann, G.S., Nichols, G.J. and Warwick, G.L.** (2010) Large Distributive Fluvial Systems: Characteristics, Distribution, and Controls on Development. *J. Sed. Res.* **80**, 167-183.
- Hazel, J.E.** (1994) Sedimentary Response to Intrabasinal Salt Tectonism in the Upper Triassic Chinle Formation, Paradox Basin, Utah. *U.S. Geological Survey Bulletin 2000-F*.

Hintze, L.F. and **Axen, G.J.** (1995) Geology of the Lime Mountain Quadrangle , Lincoln County, Nevada. Nevada Bureau of Mines and Geology, Map **129**.

Hjulstrom, F (1935) Studies of the morphological activity of rivers as illustrated by the River Fyris. *Bull. Geol. Inst. Uppsala*, **25**, 221-527.

Hodgson, N.A., Farnsworth, J. and **Fraser, A.J.** (1992) Salt-related tectonics, sedimentation, and hydrocarbon plays in the Central Graben, North Sea, UKCS. In: *Exploration Britain: Geological insights for the next decade* (Ed. R.F.P. Hardman), *Spec. Publ. Geol. Soc. London*, **67**, 31-63.

Hogg, S.E. (1982) Sheetfloods, sheetwash, Sheetflow, or ... ? *Earth-Science Reviews*, **18**, 59-78.

Hubert, J.F. and **Hyde, M.G.** (1982) Sheet-flow deposits of graded beds and mudstones on an alluvial sandflat-playa system: Upper Triassic Blomidon redbeds, St Mary's Bay, Nova Scotia. *Sedimentology*, **29**, 457-474.

Johnson, H.S. and **Thordarson, W.** (1966) Uranium Deposits of the Moab, Monticello, White Canyon, and Monument Valley Districts Utah and Arizona. U.S. Department of the Interior, Geological Survey Bulletin **1222-H**.

Jones, A.D., Auld, H.A., Carpenter, T.J., Fetkovich, E., Palmer, I.A., Rigatos, E.N. and **Thompson, M.W.** (2005) Jade Field: an innovative approach to high-pressure, high-temperature field development. In: *Petroleum Geology: North-West Europe and Global Perspectives* (Eds. A.G. Dore, B.A. Vining) *Petroleum Geology Conference series*, **6**, 269-283.

Kluth, C.F. and **DuChene, H.R.** (2009) Late Pennsylvanian and early Permian structural geology and tectonic history of the Paradox Basin and Uncompahgre uplift, Colorado and Utah. In: *The Paradox Basin Revisited: New Developments in Petroleum Systems and Basin Analysis* (Eds W.S. Houston, L.L. Wray and P.G. Moreland). *Rocky Mountain Association of Geologists Spec. Publ.*, 178-197.

Lawton, T.F. and **Buck, B.J.** (2006) Implications of diaper-derived detritus and gypsic paleosols in Lower Triassic strata near Castle Valley salt wall, Paradox Basin, Utah. *Geology*, **34**, 885-888.

Leeder, M.R., Harris, T. and **Kirkby, M.J.** (1998) Sediment supply and climate change: implications for basin stratigraphy. *Basin Res.*, **10**, 7-18.

Lindholm, R. (1987) *A practical approach to Sedimentology*, 1st Ed., Allen & Unwin, Inc, Massachusetts.

Mackey, S.D. and **Bridge, J.S.** (1995) Three-Dimensional Model of Alluvial Stratigraphy: Theory and Application. *J. Sed. Res.* **65B**, 7-31.

Mathews, W.J., Hampson, G.J., Trudgill, B.D. and **Underhill, J.R.** (2007) Controls on fluvio-lacustrine reservoir distribution and architecture in passive salt diapir

provinces: insights from outcrop analogue. *Am. Assoc. Petrol. Geol. Bull.* **91**, 1367-1403.

McKee E.D., Crosby, E.J. & Berryhill, H.J. (1966) Flood deposits, Bijou Creek, Colorado, June 1965. *J Sed. Petrol.*, **37**, 829-851.

McKie, T. (2011) Architecture and Behaviour of Dryland Fluvial Reservoirs, Triassic Skagerrak Formation, Central North Sea. In: *From Rivers to Rock Record* (eds S.K. Davidson, S. Leleu, and C.P. North) SEPM Spec. Publ. **97**, 189-214.

McKie, T and Audretsch, P. (2005) Depositional and structural controls on Triassic reservoir performance in the Heron Cluster, ETAP, Central North Sea. In: *North-West Europe and Global Perspectives – Proceedings of the 6th Petroleum Geology Conference*, 285-297.

McKie, T., Jolley, S.J. and Kristensen, M.B. (2010) Stratigraphic and structural compartmentalization of dryland reservoirs: Triassic Heron Cluster, Central North Sea. *Geol. Soc. London Spec. Publ.* **347**, 165-198.

McKie T. and Williams, B. (2009) Triassic palaeogeography and fluvial dispersal across the northwest European Basins. *Geol. J.* **44**, 711-741.

Miall, A.D. (1985) Architectural-Element Analysis: A New Method of Facies Analysis Applied to Fluvial Deposits. *Earth Sci. Rev.* **22**, 261-308.

Miall, A.D. (1996) *The Geology of Fluvial Deposits*. Springer, Berlin.

Morales, M. (1987) Terrestrial Fauna and Flora from the Triassic Moenkopi Formation of the Southwestern United States. *J. Arizona-Nevada Acad. Sci.* **22**, 1-19.

Mullens, T.E. (1960) Geology of the Clay Hills Area, San Juan County, Utah. U.S. Geological Survey Bulletin 1087-H.

Newell, A.J., Benton, M.J., Kearsy, T., Taylor, G., Twitchett, R.J., & Tverdokhlebov, V.P. (2012) Calcretes, fluvio-lacustrine sediments and subsidence patterns in Permo-Triassic salt-walled minibasins of the south Urals, Russia. *Sedimentology*, **59**, 1659-1676.

North, C.P., Nanson, G.C. and Fagen, S.D. (2007) Recognition of the Sedimentary Architecture of Dryland Anabranching (Anastomosing) Rivers. *J. Sed. Res.* **77**, 925-938.

Nuccio, V.F. and Condon, S.M. (1997) Burial and Thermal History of the Paradox Basin, Utah and Colorado, and Petroleum Potential of the Middle Pennsylvanian Paradox Formation. In: *Geology and Resources of the Paradox Basin* (eds A.C. Huffman, W.R. Lund, and L.H. Godwin), Utah Geol. Assoc. Guidebook 25.

O'Sullivan, R.B. & MacLachlan, M.E. (1975) Triassic Rocks of the Moab-White Canyon Area, Southeastern Utah. *Four Corners Geol. Soc. Guidebook*, 8th Field Conf., Canyonlands, 129-141.

- Owen, G.** (1987) Deformation processes in unconsolidated sands. In: *Deformation of sediments and sedimentary rocks* (Eds M.E. Jones, and R.M.F. Patterson), *Spec Publ Geol Soc London*, **29** 11-24.
- Owen, G.** (1996) Experimental soft-sediment deformation: structures formed by the liquefaction of unconsolidated sands and some ancient examples. *Sedimentology*, **43**, 279-93.
- Paz, M., Trudgill, B. and Kluth, C.** (2009) Salt system evolution of the Northern Paradox Basin. *Search and Discovery Article #30078*.
- Picard, M.D. and High, L.R.** (1973) Sedimentary structures of ephemeral streams. *Developments in sedimentology* **17**, Elsevier Sci. Publ. Co., Amsterdam, Netherlands.
- Prochnow, S.J., Atchley, S.C. Boucher, T.E., Nordt, L.C. and Hudec, M.R.** (2006) The influence of salt withdrawal subsidence on palaeosol maturity and cyclic fluvial deposition in the Upper Triassic Chinle Formation: Castle Valley, Utah. *Sedimentology*, **53**, 1319-1345.
- Rahn, P.H.** (1967) Sheetfloods, Streamflood, and the formation of Pediments. *Ann. Assoc Am. Geog.* **57**, 593-604.
- Rasmussen, L. and Rasmussen D.L.** (2009) Burial History Analysis of the Pennsylvanian Petroleum System in the Deep Paradox Basin Fold and Fault Belt, Colorado and Utah. In: *The Paradox Basin Revisited: New Developments in Petroleum Systems and Basin Analysis* (Eds W.S. Houston, L.L. Wray and P.G. Moreland). *Rocky Mountain Association of Geologists Spec. Publ.*, 24-94.
- Reid, I., Laronne, J.B. and Powell, D.M.** (1998) Flash-flood and bedload dynamics of desert gravel-bed streams. *Hydrol. Process.*, **12**, 543-557.
- Rumsby, B.T., and Macklin, M. G.** (1994) Channel and Floodplain Response to recent abrupt climate change: the Tyne Basin, Northern England. *Earth Surf. Process. Landf.*, **19**, 499-515.
- Rodríguez-López, J.P., Lies, C.L., Van Dam, J. La Fuente, P., Arlegui, L., Ezquerro, L., and De Bore, P.** (2012) Aeolian construction and alluvial dismantling of a fault-bounded intracontinental aeolian dune field (Teruel Basin, Spain); a continental perspective on Late Pliocene climate change and variability. *Sedimentology*, **59**, 1536-1567.
- Rust, B.R.** (1981) Sedimentation in an arid-zone anastomosing fluvial system: Cooper's Creek, Central Australia. *J. Sedim. Petrol.*, **51**, 745-755.
- Rust, B.R. and Legun, A.S.** (1983) Modern anastomosing-fluvial deposits in arid Central Australia, and a Carboniferous analogue in New Brunswick, Canada. *Spec. Publ. Int. Assoc. Sediment*, **6**, 385-392.

- Shoemaker, E.M. and Newman, W.L.** (1959) Moenkopi Formation (?Triassic and Triassic) in Salt Anticline Region, Colorado and Utah. *Am. Assoc. Petrol. Geol. Bull.*, **42**, 1835-1851.
- Smith, R.I., Hodgson, N. and Fulton, M.** (1993) Salt controls on Triassic reservoir distribution, UKCS Central North Sea. In: *Petroleum Geology of Northwest Europe: Proceedings of the 4th Conference* (Ed. J.R. Parker), *Geol. Soc. London*, 547-557.
- Stewart J.H.** (1959) Stratigraphic relations of Hoskinnini Member (Triassic?) of Moenkopi Formation on Colorado Plateau. *Am. Assoc. Petrol. Geol. Bull.*, **43**, 1852-1868.
- Stewart J.H., Poole, F.G., Wilson, R.F. and Cadigan, R.A.** (1972) Stratigraphy and Origin of the Triassic Moenkopi Formation and Related Strata in the Colorado Plateau Region. *Geological Survey Professional Paper 691*.
- Stanesco, J.D., Dubiel, R.F. and Huntoon, J.R.** (2000) Depositional Environments and Palaeotectonics of the Organ Rock Formation of the Permian Cutler Group, Southeastern Utah. In: D.A. Sprinkel, T.C. Chidsey Jr., P.B. Anderson (eds) *Geology of Utah's Parks and Monuments, Utah Geological Association Publication 28*.
- Stokes, W.L.** (1987) *Geology of Utah*. Utah Geological and Mineral Survey, Occasional Paper 6.
- Sundborg, A.** (1956) The River Klaralven: a study of fluvial processes. *Geogr. Annlr.* **38**, 127-316.
- Thamó-Bozsó, E., Kercksmár, Z., and Annamária, N.** (2002) Tectonic control on changes in sediment supply; Quaternary alluvial systems, Körös sub-basin, SE Hungary. In: *Sediment flux to Basins: Causes, Controls and Consequences* (Eds S.J. Jones and L.E. Frostick). *Geol. Soc. London, Spec. Pub*, **191**, 37-53.
- Thaden, R.E., Trites, A.F. and Finnell, T.L.** (1964) Geology and ore deposits of the White Canyon area, San Juan and Garfield Counties, Utah. *U.S. Geol. Surv. Bull.* **1125**.
- Tooth, S.** (1999a) Floodouts in central Australia. In: *Varieties of Fluvial Form* (Eds A.J. Miller and A. Gupta), pp. 219–247. John Wiley & Sons, New York.
- Tooth, S.** (1999b) Downstream changes in floodplain character on the Northern Plains of arid central Australia. *Spec. Publs. Ass. Sediment.* **28**, 93-112.
- Tooth, S.** (2000) Downstream changes in dryland river channels: the Northern Plains of arid central Australia. *Geomorphology*, **34**, 33-54.
- Trudgill, B.D.** (2011) Evolution of salt structure in the northern Paradox Basin: controls on evaporitic deposition, salt wall growth and supra-salt stratigraphic architecture. *Basin Res.*, **23**, 208-238.

Trudgill B.D. and Paz, M. (2009) Restoration of Mountain Front and Salt Structures in the Northern Paradox Basin, SE Utah. In: *The Paradox Basin Revisited: New Developments in Petroleum Systems and Basin Analysis* (Eds W.S. Houston, L.L. Wray and P.G. Moreland). *Rocky Mountain Association of Geologists Spec. Publ.*, 132-177.

Tunbridge, I.P. (1981a) Sandy high-energy flood sedimentation – some criteria for recognition, with an example from the Devonian of SW England. *Sediment. Geol.* **28**, 79-95.

Tunbridge, I.P. (1981) Old Red Sandstone Sedimentation – An example from the Brownstones (highest Lower Old Red Sandstone) of South Central Wales, *Geol.J.*, **16**, 111-124.

Venus, J.H. (2012) Tectono-stratigraphic evolution of fluvial and aeolian systems in a salt mini-basin province during changing climatic conditions: Permian Undifferentiated Cutler Group, South East Utah, USA. Unpublished *PhD Thesis*, University of Leeds.

Ward, L.F. (1901) Geology of Little Colorado Valley. *Am. J. Sci.*, **12**, 401-413.

Weismann, G.S. Hartley, A.J. Nichols G.J., Scuderi, L.A., Davidso, S.K. and Owen, A. (2011) Predicted Progradational Signatures of Distributive Fluvial Systems (DFS). *Am. Geophys. Union*, #EP21B-0702.

Williams G.E. (1970) The Central Australian Stream Floods of February-March 1967. *J. Hydrol.* **11**, 185-200.

Williams G.E. (1971) Flood deposits of the Sand Bed Ephemeral Streams of central Australia. *Sedimentology*, **17**, 1-40.

Figure Captions

Fig 1. Paradox Basin Overview. (a) Regional map of the Paradox Basin and location of the study areas in relation to areas of likely sediment provenance of the Moenkopi Formation. Modified after Banham & Mountney (*in press*).

Fig 2. Paradox Basin Overview. (b) Regional stratigraphic column and paleocurrent summary data. Column depicts the average thickness of the various stratigraphic units within the Paradox Basin, and average thickness of the Moenkopi Formation in the three studied basins of the Salt Anticline Region and Copper Point, White Canyon Region. Palaeocurrent summary data for each studied mini-basin and White Canyon Region are plotted as a rose diagram vector mean (Vm) and vector magnitude (Vg) are: Fisher Basin, Vm= 305°, Vg=0.91, n=88; Parriott Basin,

Vm=303°, Vg=0.85, n=57; Big Bend, Vm= 292°, Vg=0.77, n=32; Wave Ripples, SAR, Vm=052°, Vg=0.73, n=62; Copper Point, WCR, Vm=333°, Vg=0.89, n=56. After Trudgill (2011) and Banham & Mountney, *in press*.

Fig.2. Overview location maps. (a) Salt Anticline Region study area map depicting the location of salt walls and mini-basins in relation to the present-day topography. Map centre: 38.70°N, 109.324°W, geodesic syst em: WGS 84 (modified after Banham & Mountney, *in press*). (b) White Canyon Region study area map. Map centre 37.566°N, 110.233°W, geodesic syst em: WGS 84. The location of measured vertical log profiles is indicated.

Fig. 3. Representative lithofacies of the Moenkopi Formation in the Salt Anticline Region (SAR) and White Canyon Region (WCR). See Table 1 for explanation of lithofacies codes. Black borders indicate photograph was taken in SAR, green border indicate WCR. Note that all depicted facies occur commonly in both areas, unless otherwise stated. (a) Trough cross-bedded sandstone (Fxt) with intraformational clasts (Fci). 1: Erosive base 2: Medium- to coarse- grained trough cross-bedded sandstone with a high proportion of intraformational clasts (which are mostly removed by erosion) 3: Intraformational clasts are angular to sub-rounded and <30 mm in size. (b) Horizontally laminated sandstone (Fh). 1: repeating small-scale fining upwards cycles 2: coarse-grained base of fining-up cycle. (c) Trough cross-bedded sandstone (Fxt). 1: Large scale cross-bedding is indicative of larger bedforms that typically develop in main channels. 2: Thin foresets within trough. 3: Grain size is typically medium-grained, although sporadic floating pebbles do occur (both intra- and extraformational). (d) High-angle planar cross-bedding (ha Fxp). 1: High angle tangential terminating foresets indicate direction of palaeoflow. 2: Erosive base foresets result from successive dunes migrating over the previous dune at sub-critical angles of climb. (e) Climbing ripple-strata (Frc) 1: Climbing ripple stratification in sets composed of fine- to medium-grained sandstone. 2: Positive, subcritical angle of climb. 3: Direction of Palaeoflow. (f) Wave-ripple laminated sandstone (WR). 1: Ripple forms preserved on upper bedding surfaces. In section these can exhibit combinations of chevron up-building, and draping of foresets onto ripple crests. 2: Some examples of asymmetric ripples indicate mixed uni- and bi-directional flow regime, which are typical of wind shear influence on shallow water. (g) Gypsum-clast-

bearing unit; matrix supported (FGm). 1: Gypsum clasts are sub-angular: indicative of short transport distance. 2: Matrix-supported nature of sets indicates deposition by debris flow or water flow. 3: Pebble-grade clast horizon overlain by coarse-grained granulestone of gypsum micro-conglomerate, indicating disaggregation of larger clasts in higher energy flows, or possibly indicative of longer transport distances. (h) Gypsum-clast-bearing unit; clast supported (FGc). 1: Clast-supported gypsum horizon indicates close proximity to the source of gypsum detritus. 2: Gypsum clast-bearing intervals are discrete in nature, indicating episodic availability of diaper-derived detritus. (i) Preserved ripple. 1: Preserved asymmetric ripple crest, exhibiting a stoss and lee side of ripple. 2: Internal lamination, indicating direction of ripple migration. 3: Erosive base where successive migrating ripple has eroded and reworked pre-existing ripple strata. (j) Trough cross-bedded sandstone (Fxt). 1: lee side of dunes preserved as laminations which terminate tangentially to against coset beneath. 2: bounding surface defining top and base of coset. 3: coset, composed of cross-strata. (k) Subcritical to critical angle climbing-ripple strata (Frc). 1: Variable angle of climb indicates changing rate in sediment accumulation. 2: sigmoidal laminations indicate complete preservation of migrating ripple forms. 3: Critical angle of climb, where stoss-sides of ripples are preserved. (l) Massively bedded, graded sandstone (Fm). 1: Coarse, poorly-sorted, angular sand grains 2: Fining up cycles, indicating multiple phases of deposition from waning flows, or a single pulsing flow. (m) Horizontal interbedded siltstone and sandstone (Fhiss) 1: thicker sand lens (composed of massive bedded sandstone) preserved within a succession of heterolithic strata. 2: typical expression of heterolithic strata composed of interbedded sandstones and argillites, representing a deposition from a waning flow. (n) Horizontal interbedded siltstone and sandstone (Fhiss) 1: Sand-prone Fhiss, characterised by a higher proportion of sand preserved. 2: Sand-poor Fhiss, characterised by lower proportion of sand preserved. Both represent variations in sediment supply to this specific location, which can be controlled by sediment supply rates or autocyclic processes. (o) Horizontal interbedded siltstone and sandstone (Fhiss) 1: Climbing-ripple strata preserved in heterolithic succession, indicating bed-load transport. 2: succeeding siltstone horizon indicates progressive decrease in flow velocity after accumulation of climbing-ripple strata during initial stage of sediment deposition. 3: Palaeocurrent direction. (p) Crystalline gypsum horizon (GC) Crystalline gypsum horizon, in weathered form.

Fig. 4. (a) Representative sedimentary logs from the three studied mini-basins in the Salt Anticline Region. Fisher basin section is from Richardson Amphitheater mile 25.5; Parriott basin sections are Parriott Mesa south east (sand-poor part of succession) and The Priest (sand-prone part of succession); Big Bend basin section is from Big Bend Campsite C. (b) Representative sedimentary logs from the White Canyon Region. See Fig. 4a for facies key.

Fig 5. Representative architectural elements from the Salt Anticline Region (SAR). (a) Multi-storey, multi-lateral elements with heterolithic sheet-like elements. (b) Single-store, multi-lateral channel element. (c) Conical de-watering structure. Tape measure is 1 m. (d) Close-up view of sheet-like heterolithic strata. Representative architectural elements from the White Canyon Region (WCR). (e) Multi-storey, multi-lateral elements with heterolithic sheet-like elements. Note chute element nested in sand-prone portion of sheet-like heterolithic element. (f) Multi-storey, multi-lateral channel elements nested in sand-prone sheet-like heterolithic channel elements. (g) Margin of a channel element, where the channel element has incised into the underlying sheet-like heterolithic element.

Fig.6. Representative architectural elements, depicting generalised geometries and internal facies composition of the principal architectural elements of the Moenkopi Formation.

Fig. 7. Three-dimensional multi-element deposition models depicting confined- and non-confined flow architectural elements.

Fig 8. Generalised deposition model depicting relationships between confined & non-confined fluvial elements.

Fig 9. Generalised deposition model for the Salt Anticline Region. Model depicts the relationship of fluvial elements to the uplifted Fisher Valley salt wall, which acted to isolate the neighbouring Fisher and Parriott mini-basins.

Fig 10. Changes in stratigraphic expression between different mini-basins for members of the Moenkopi Formation in the Salt Anticline Region. See figure 2 for locations.

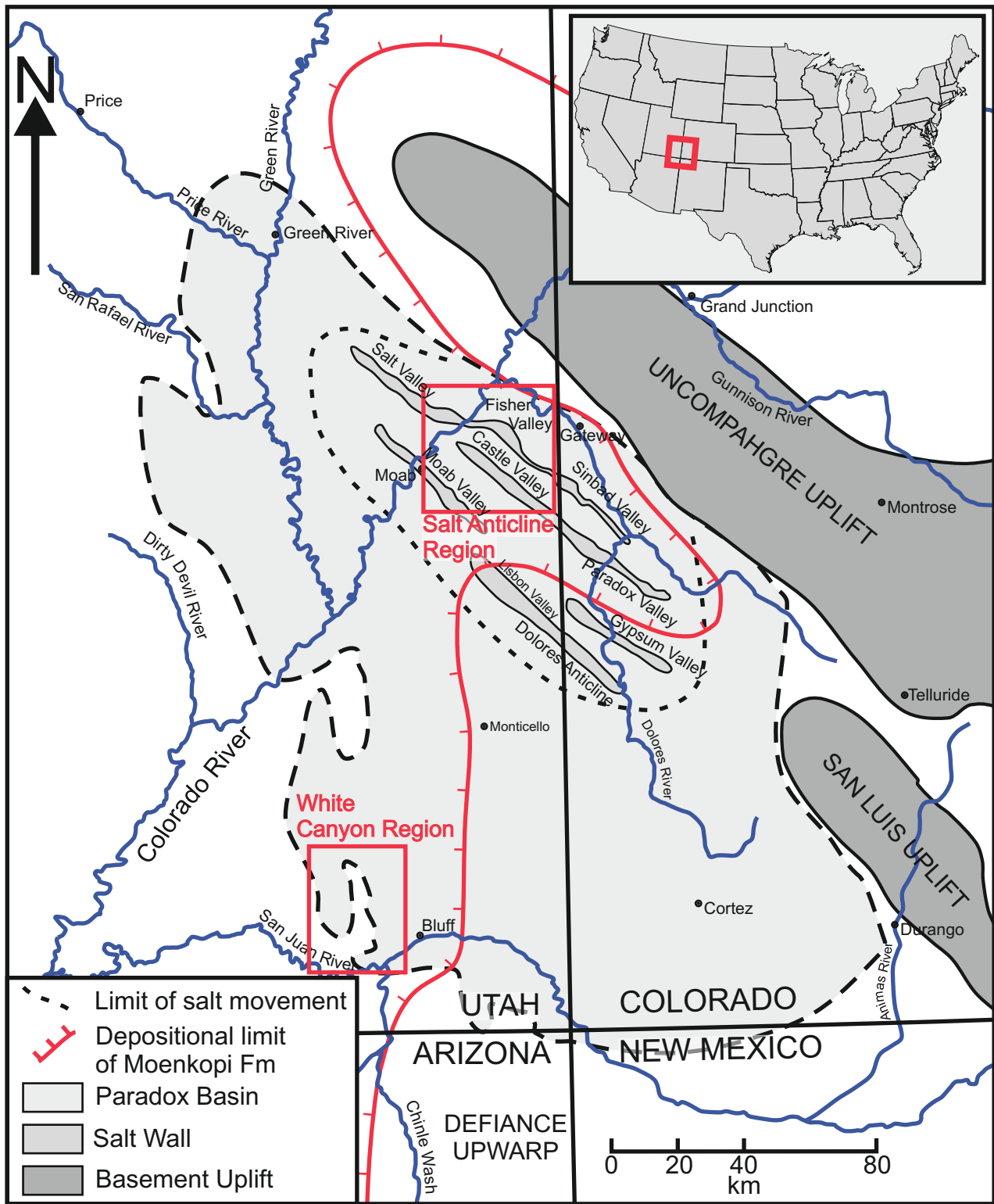
Fig. 11. Generalised deposition model for White Canyon area. Model depicts the relationship of fluvial elements beyond the region of halokinetic influence.






Fig 12. Stratigraphic features of the Moenkopi Formation in the White Canyon Region.

Fig 13. Regional summary depositional model for the Monekopi Formation. Modified in part from Stuart *et al.* (1972), Blakey (1974), Stanesco *et al.* (2000) and Blakey & Ranney (2008).

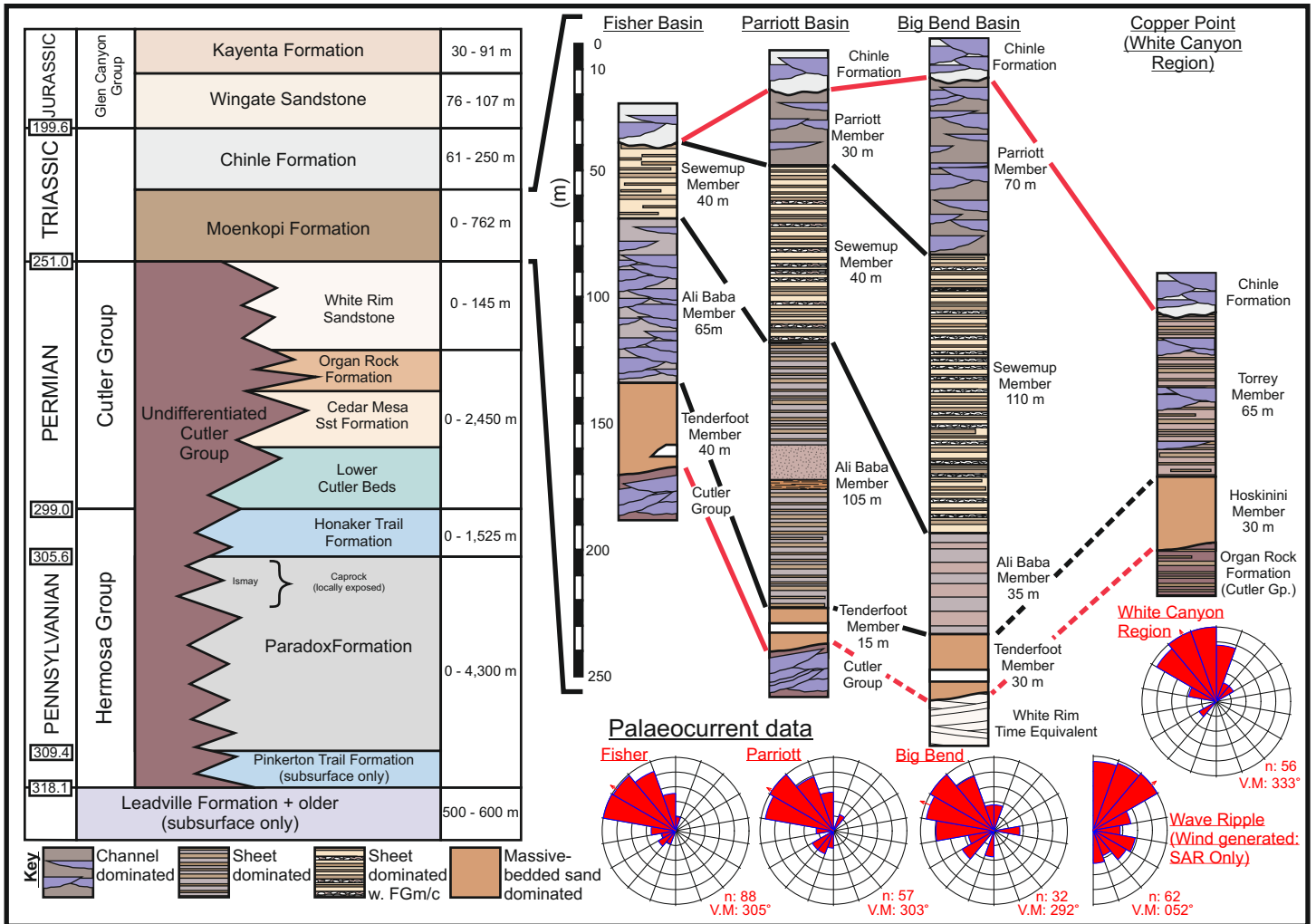
Code	Lithofacies	Description	Interpretation
Fce	Extraformational conglomerate	Crudely-bedded (sometimes trough cross-bedded), matrix or clast supported, poorly sorted with rounded clasts. Matrix is medium sand to granule grade. Clasts composed of crystalline basement rocks.	Represents immature material derived from the Uncompahgre Highlands.
Fci	Intraformational conglomerate	Crudely bedded, matrix or clast supported, very poorly sorted with angular clasts. Matrix can be fine- to coarse-sand. Clasts are composed of locally derived siltstone or sandstone.	Represents the entrainment and reworking of locally derived sediment. Can occur as basal lags or as channel fill.
Fxt	Trough cross-bedded sandstone	Fine-sand to granule grade, moderate- to poorly-sorted and sub-angular to sub-rounded. Beds are typically 0.3 to 2 m thick. Sets can have coarse-grained lags of gravel.	Represents down-channel migration of sinuous-crested sand or gravel meso-forms (dune scale).
ha Fxp	High-angle planar cross-bedded sandstone	Fine-sand to granule grade, moderate- to poorly-sorted and sub-angular to sub-rounded. Beds are typically 0.3 m to 1 m thick. This facies is defined by planar-tabular sets that are tangential to the set base. Subcritical angle of climb.	Represents sinuous- or straight-crested sand (rarely gravel) meso-forms (dune scale) migrating down channel.
la Fxp	Low-angle planar cross-bedded sandstone	Fine-sand to granule grade, moderate- to poorly-sorted and sub-angular to sub-rounded. Beds are typically 0.3 m to 1 m thick. This facies is defined by planar-tabular sets that are asymptotic to the set base.	Represents cross-flow migration of sandy, laterally accreting macro-forms. Typically a component of point bars, or mid-channel bars.
Frc/Fxl	Climbing-ripple strata and trough cross-laminated sandstone	Very-fine to medium sand, moderate- to well-sorted, sub-rounded to rounded. Beds typically 50 mm to 2 m thick. Ripple strata typically climb at angles <10° (subcritical), but can climb at supercritical angles (>15°). Ripple forms are sinuous-crested (Fxl) or undetermined (straight- or sinuous-crested) (Frc).	Represents down-flow migration of sandy micro-forms in either channelised or non-confined environments in waning flow regimes.
Fh	Horizontally laminated sandstone	Very-fine to fine sand, moderate to well-sorted, sub-rounded to rounded. Some examples are medium- to coarse-sand and angular grains. 2 to 7 mm laminations in sets > 50 mm thick. Primary current lineation on bedding surfaces.	Deposited under upper-flow regimes either in channelised or partially/non-confined sheet-like units. Coarse-grained examples are associated with partially confined flows.
Fm	Massive (structureless) sandstone	Fine- to medium-sand, moderate- to poorly-sorted, sub-angular to rounded. Bed thickness ranges from 0.1 to 2 m thick. Beds may be normally graded.	Represents rapid deposition of sand from suspension. Grading (where present) indicates gradual waning of flow velocity.
Fd	Deformed bedding	Very-fine to medium-sand, moderately sorted, sub-angular to sub-rounded. Set thickness ranges from 0.1 to 1.7 m. Deformed bedding includes structures such as slumps and water escape structures.	Water escape structures represent water loss via infiltration through less permeable layers in response to increase in pore-water pressure caused by sediment loading. Slump structures may indicate sediment movement down-slope.
FGm/c	Gypsum clast horizon (Matrix and clast supported)	10 to 150 mm diameter clasts with fine-grained sand matrix. Generally very-poorly sorted, with rounded gypsum clasts that can be either matrix or clast supported. Gypsum clasts are rarely mixed with intraformational clasts and very rarely with extraformational clasts.	Discrete beds of gypsum-clast-bearing strata; indicate episodic reworking of diapir-derived detritus. These strata record episodes when salt walls had breached the land surface, resulting in the availability of gypsum material for reworking.

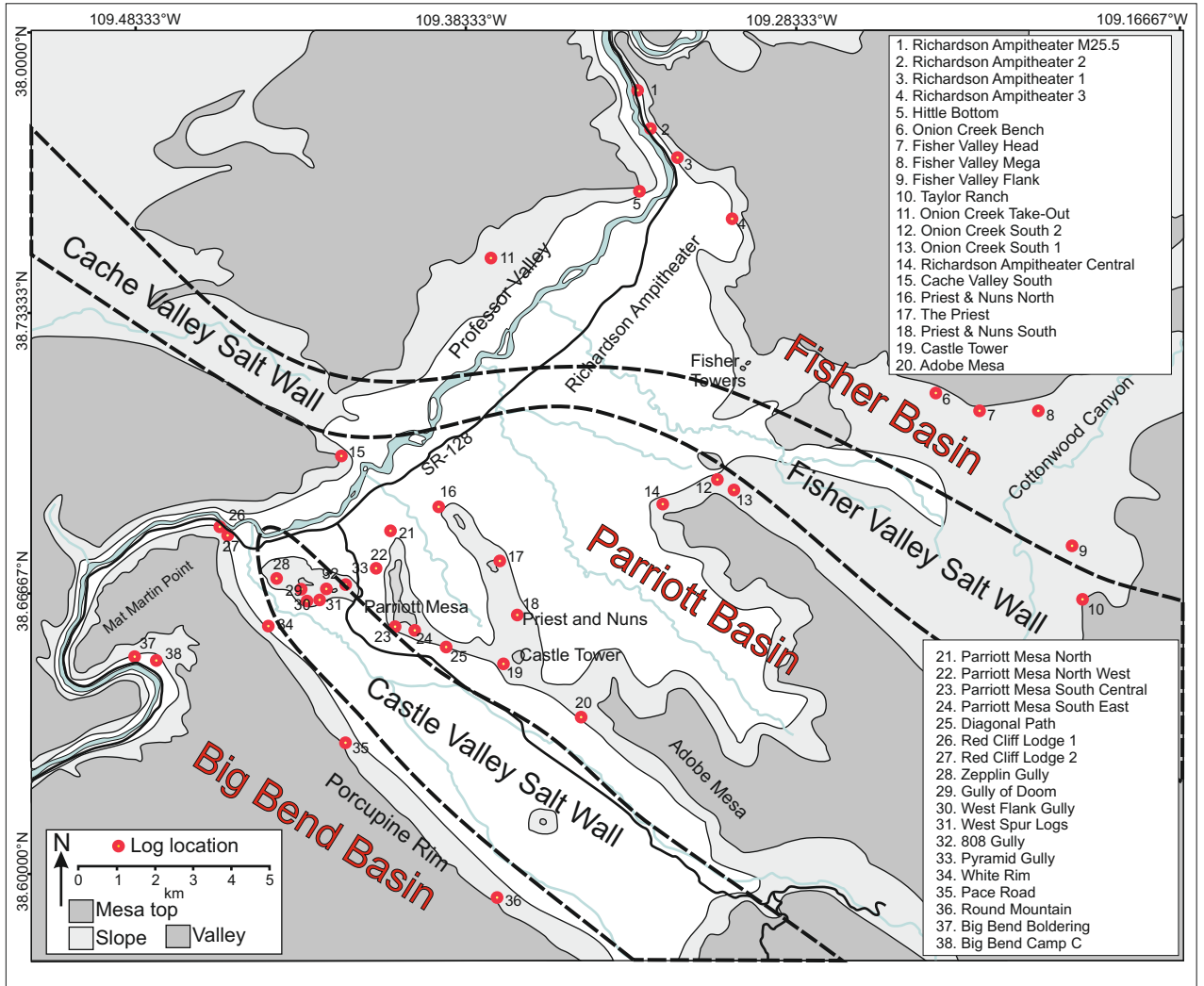
Fhiss	Horizontally interbedded siltstone and sandstone	Fine- to coarse-sand, moderately sorted, interbedded with homogeneous or laminated siltstone. Sandstone may be characterised by sedimentary structures seen in facies Fh , Fm , Frc/Fxl , WR and rarely Fci . Desiccation cracks in-filled with homogeneous sandstone are common.	Represents multiple non-confined flow events where a waning flow resulted in accumulation of progressively finer-grained sediment, with associated sedimentary structures.
WR	Wave-rippled sandstone	Very-fine to fine-sand, poorly- to moderately-sorted, sub- angular to sub-rounded. Occurs in sets 10 mm to 0.3m thick. Typically symmetrical ripple forms but can co-exist with asymmetric ripples. Ripple crests are generally parallel and continuous over long distances relative to wavelength.	Represents micro-forms generated in response to oscillating water in puddles or shallow ponds, usually in response to wind action. Slight asymmetry of some ripple forms may indicate slight current modification.
GC	Crystalline gypsum	1 to 2.5 m-thick homogenous or laminated gypsum bed (laminations may be convoluted). Gypsum may have a saccaroidal form or occur as flakey sheets. Some layers near the top of the bed can contain clinofolds.	Accumulation of gypsum by precipitation of saline water, potentially in a restricted basin. Clinofolds are interpreted to have been generated by aeolian dune-form migration (Lawton & Buck 2006) in the aftermath of episodes of desiccation.
Scls	Crenulated sandstone	Fine- to medium-sand, sub-angular to sub-rounded. Beds are characterised by discordant "crinkly" laminations.	Represents disruption of pre-existing sedimentary structures by water movement driven by capillary action (cf. Goodall <i>et al.</i> , 2000).
SGb	Gypsum-bound sandstone	Typically fine- to medium-sand (rarely coarse), poorly-sorted. Gypsum-bound sandstone is typically massively bedded and has a pervasive gypsum cement.	Origin is linked to throughflow of saline fluid and subsequent precipitation of gypsum in the pore space as water evaporated at the ground surface.

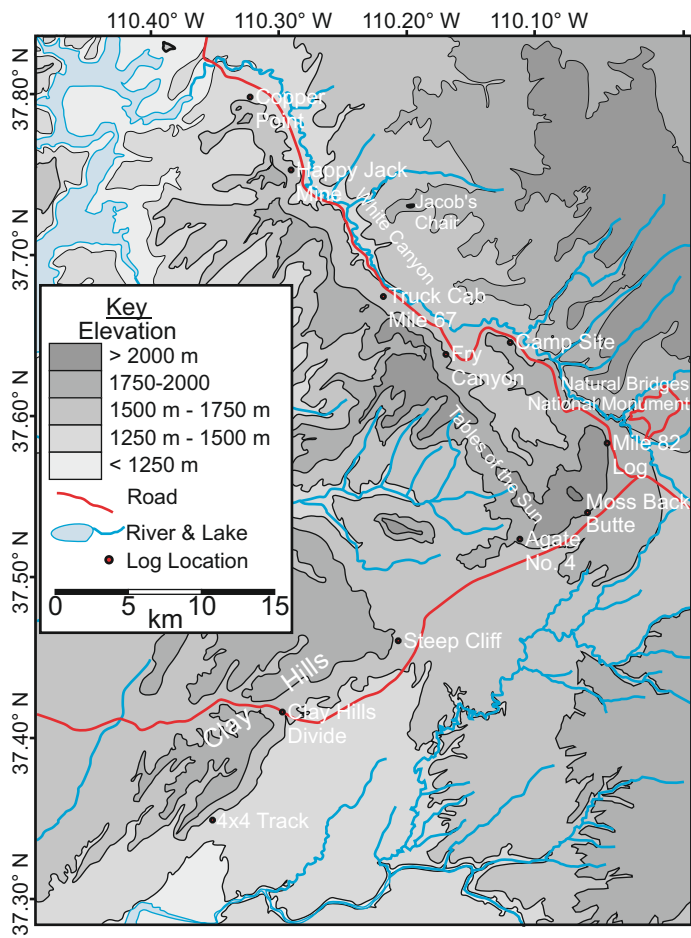


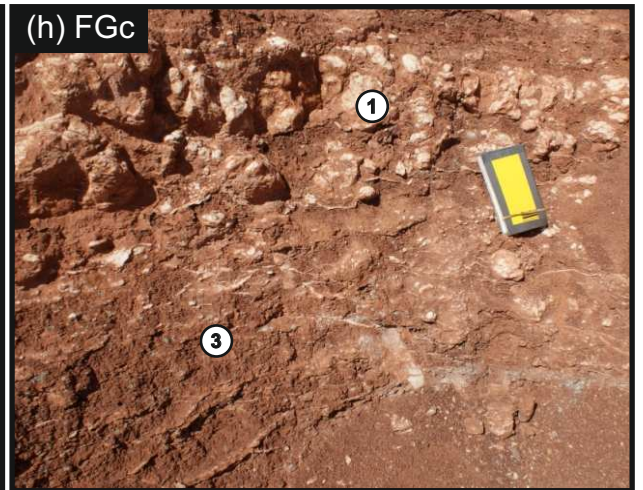
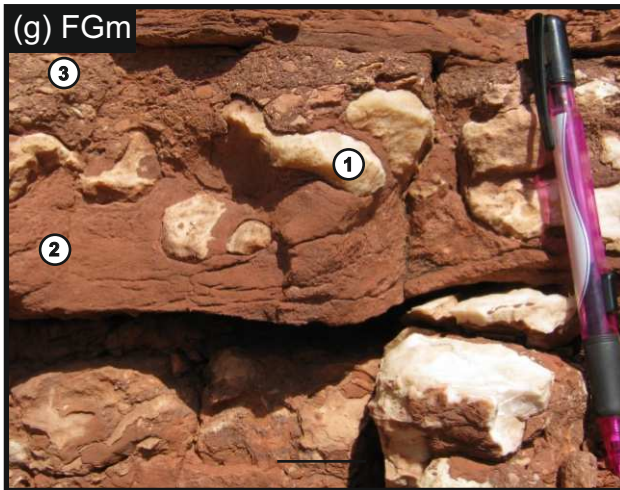
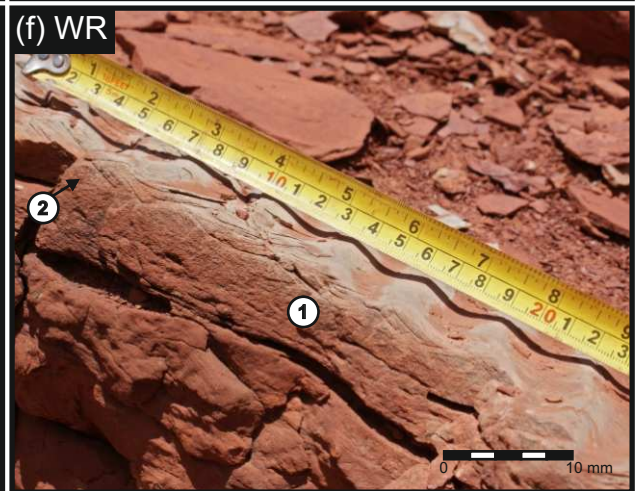
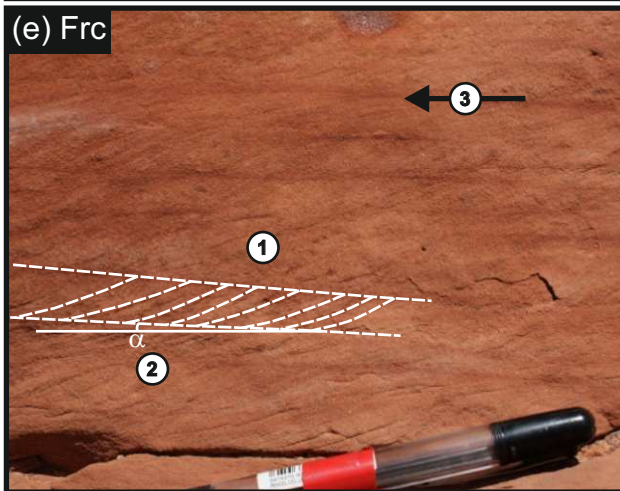
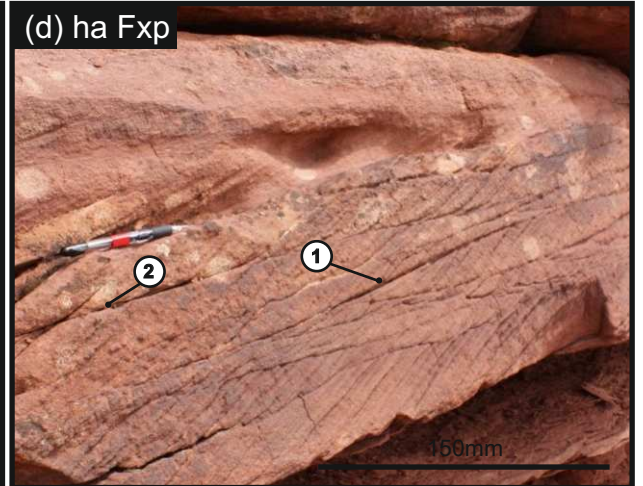
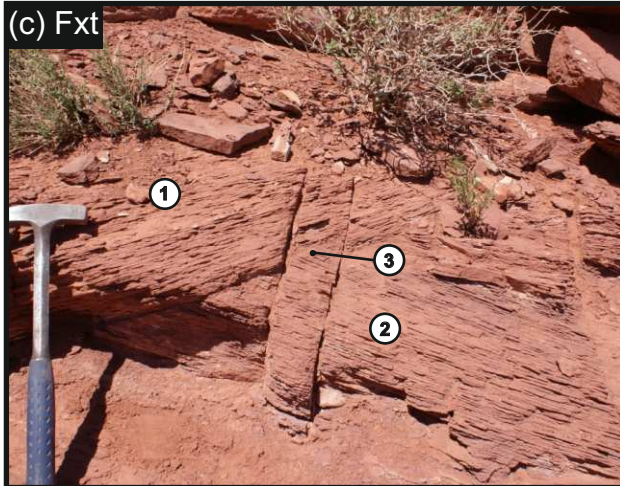
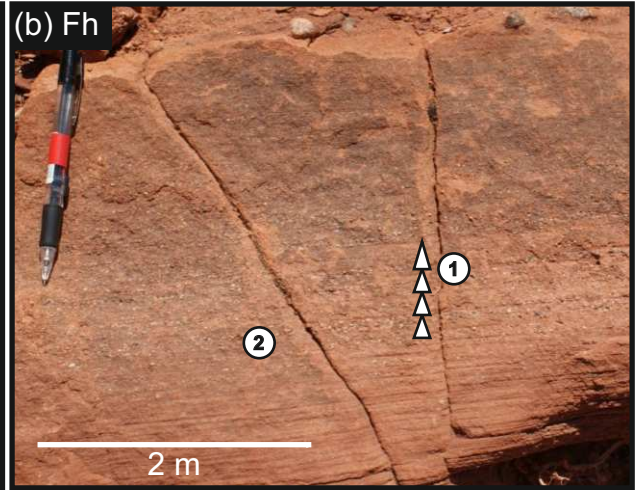
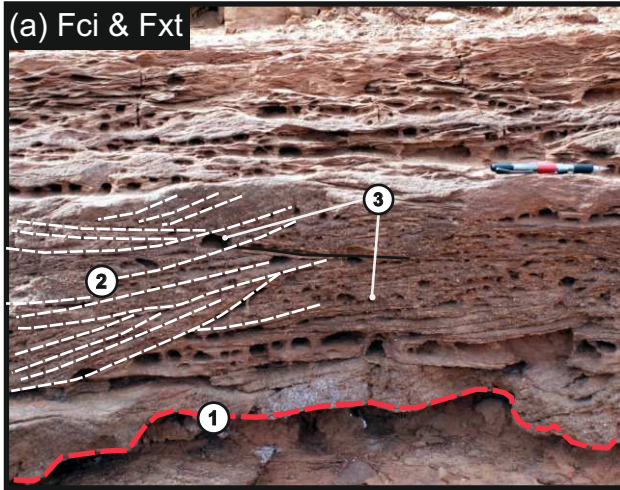
-  Limit of salt movement
-  Depositional limit of Moenkopi Fm
-  Paradox Basin
-  Salt Wall
-  Basement Uplift

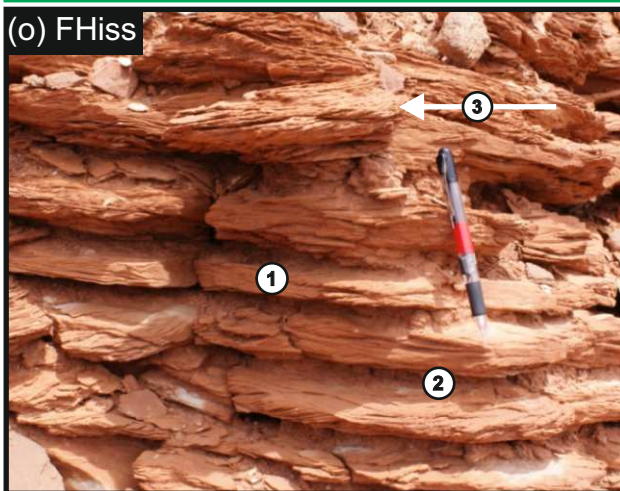
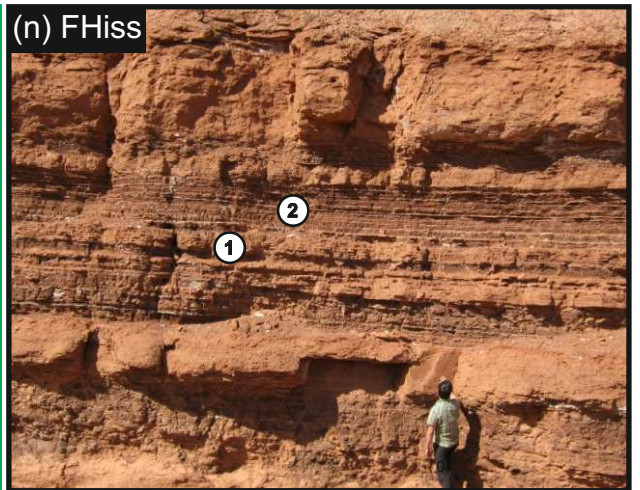
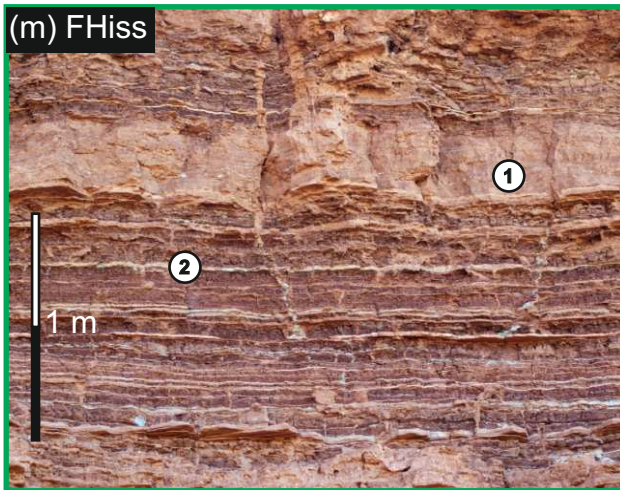
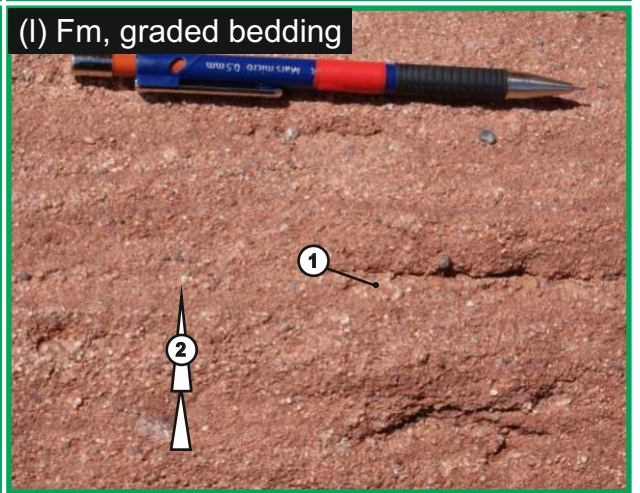
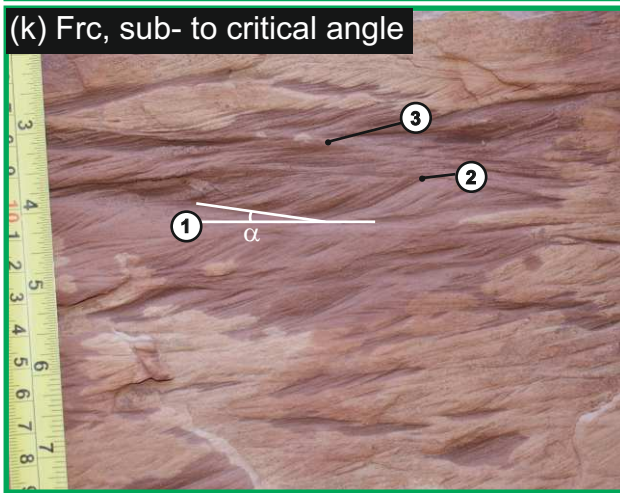
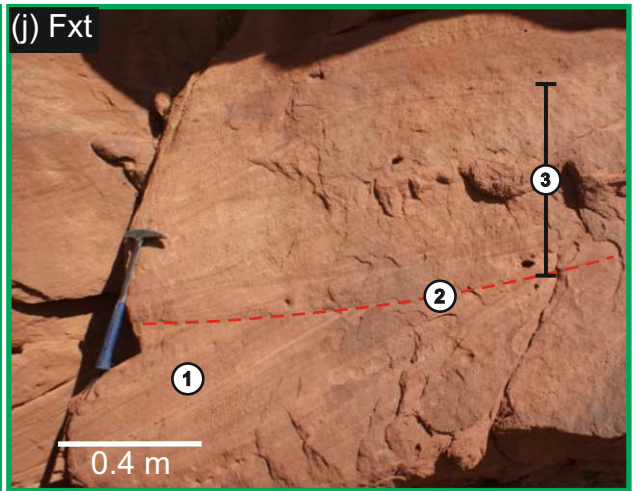
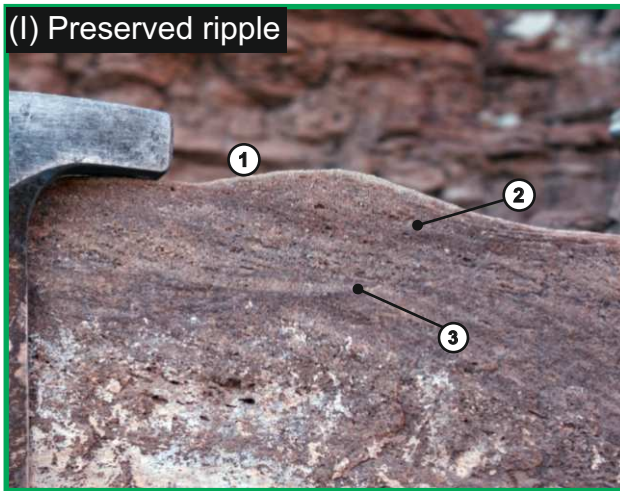
0 20 40 80
km



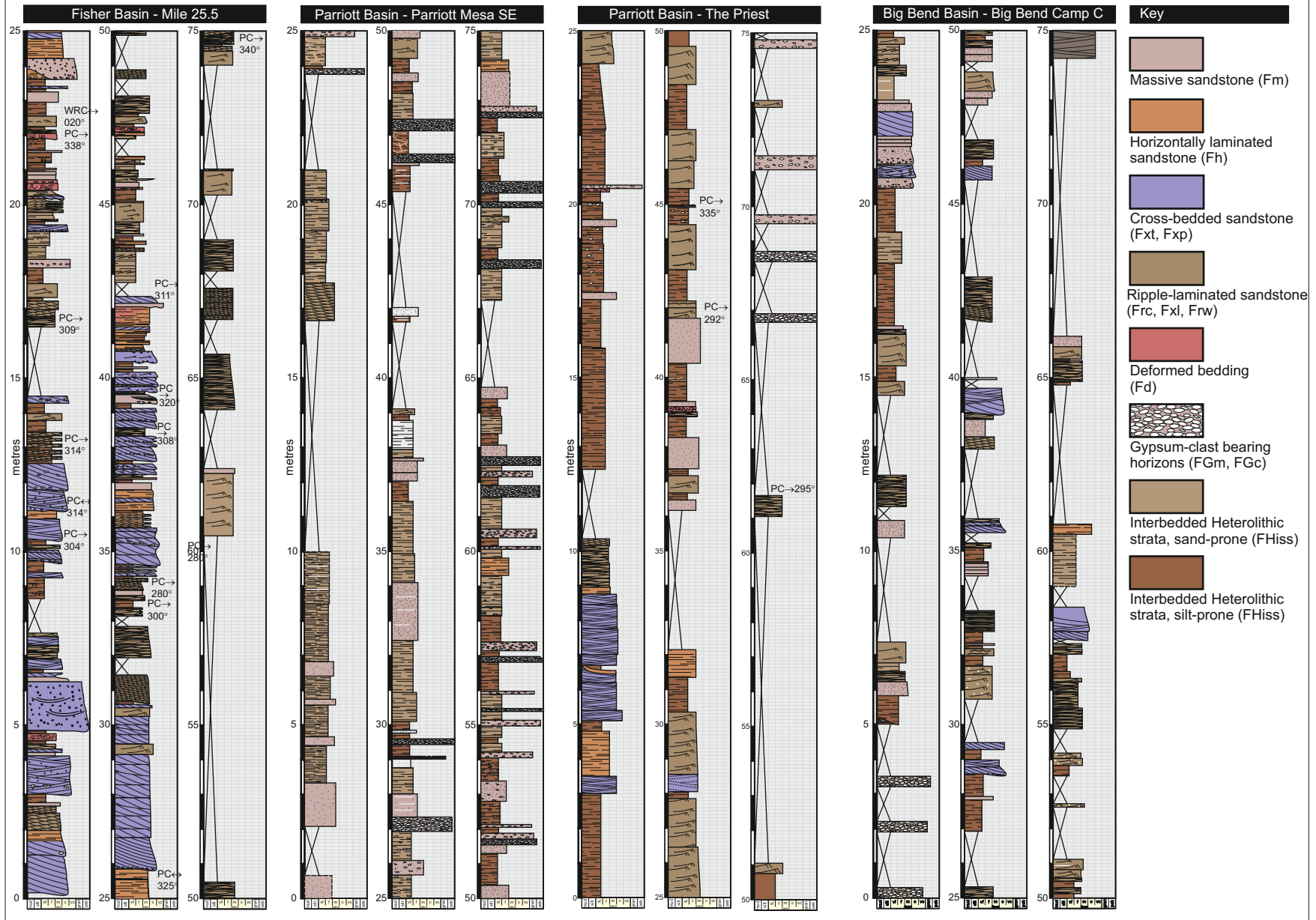




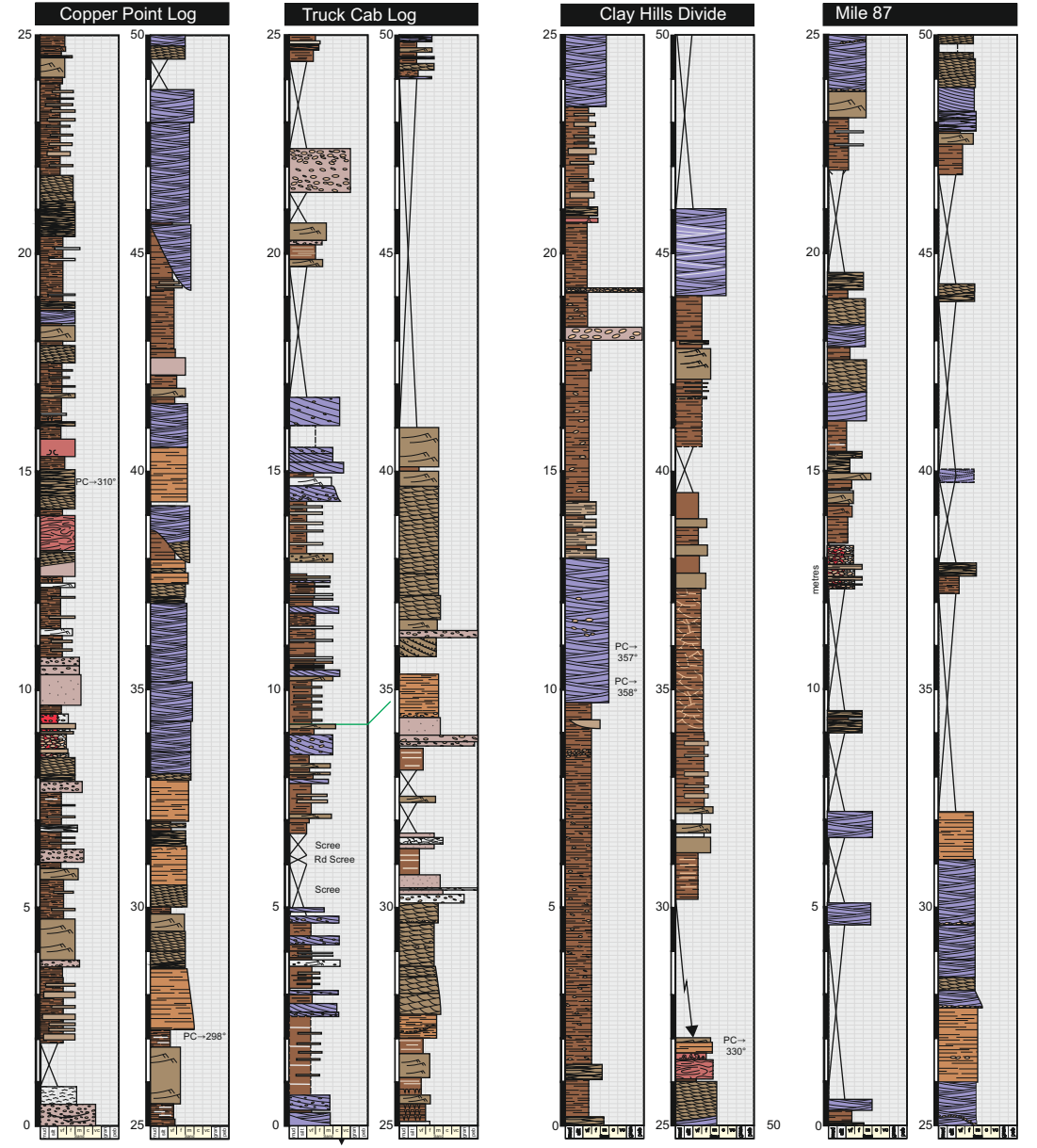


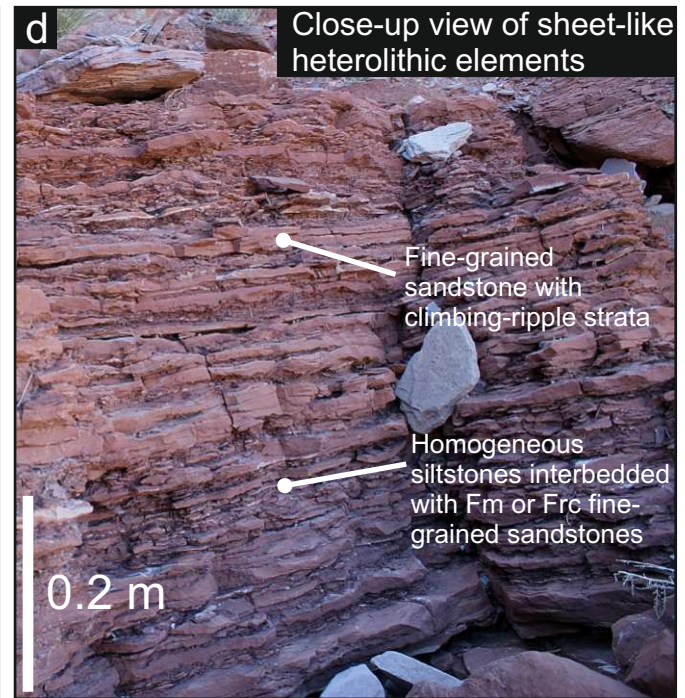
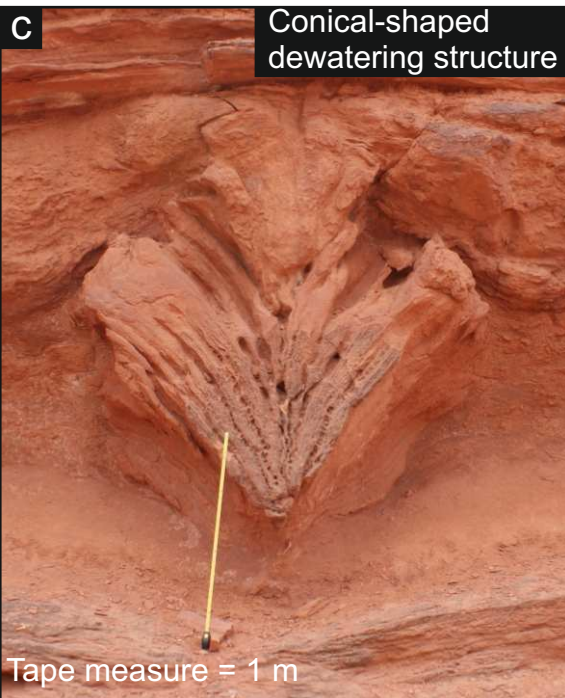


Representative Sedimentary Logs - Salt Anticline Region

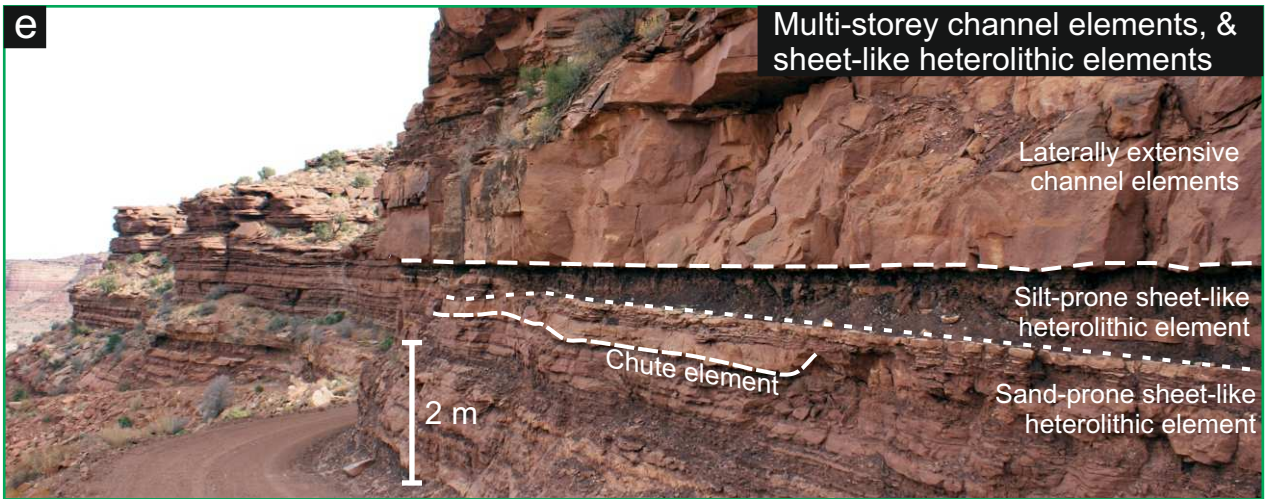


Representitive Sedimentary Logs - White Rim Region





e



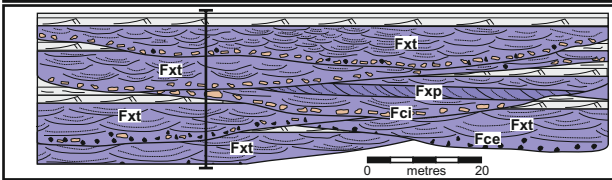
f



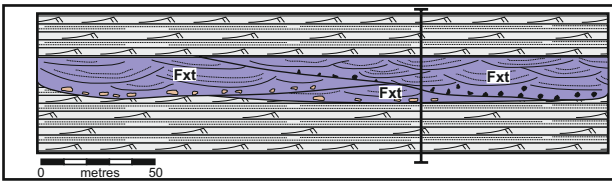
g



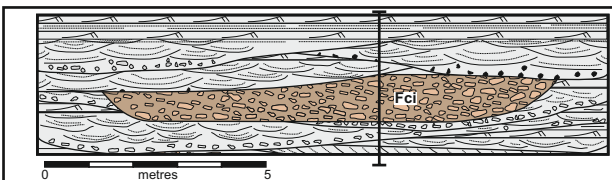
Architectural elements: typical geometry, facies successions and associations observed in outcrop



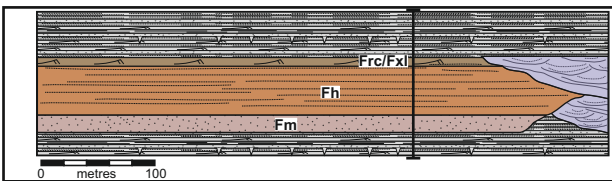
Multi-storey, multi-lateral amalgamated channel-fill complex
F1
 Vertically and laterally amalgamated, generally restricted to the Ali Baba and Parriott Members; most prevalent in the Fisher Basin where sediment supply was greatest.



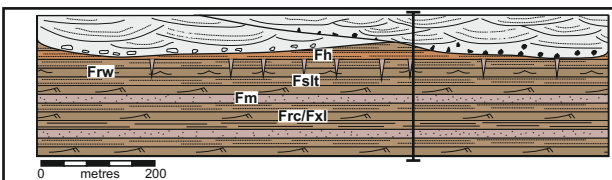
Single-storey, multi-lateral channel-fill complex
F2
 Laterally but not vertically amalgamated; common in the Sewemup Member and the central parts of the Parriott Basin in the Parriott Member; infill finer-grained than that of F1 elements, possibly reflecting accumulation in more distal locations.



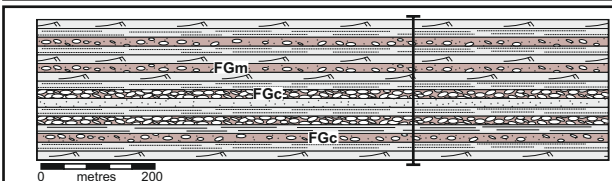
Single-storey, unilateral channel element (intraformational clast-infill)
F3
 Associated with F1 & F2 elements in locations adjacent to salt walls; fill is typically of intraformational clasts up to 0.2 m in diameter; clasts derived locally, either by physical reworking of exposed salt-wall flanks or of overbank areas.



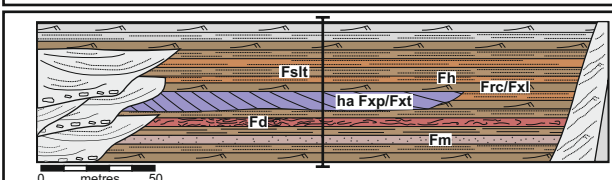
Massive (structureless) & horizontally laminated channel-fill element
F4
 Occur laterally adjacent to F1 & F2 elements in locations proximal to salt walls; composed of massively-bedded sand at base (Fm); overlain by horizontally-laminated sand (Fh); implies high-energy, initially erosional flows; rapid sedimentation via suspension settling.



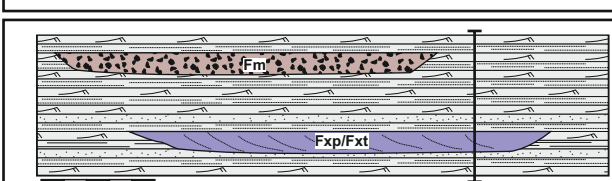
Sheet-like heterolithic element
F5
 Laterally extensive sheet-like bodies composed of interbedded silts and fine-grained sands; deposited in response to the dispersion of non-confined flood waters across floodplain areas; floods sourced via overflow from main channels or via overland flow during rain storm events.



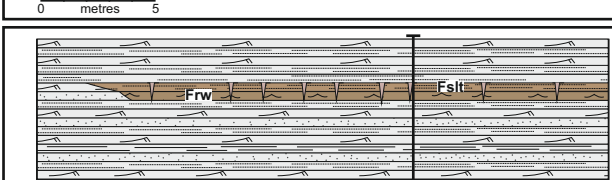
Gypsum-clast bearing element
F6
 Predominantly occur as sheet-like conglomeratic elements interbedded with sheet-like heterolithic elements (F5); common in the vicinity of the Castle Valley salt wall; reworking of gypsum detritus derived from exposed and eroding salt walls by non-confined flood waters (high-energy flows).



Partially-confined over-spill elements
F7
 Generally sheet-like form though with minor scour surfaces in some cases; common in areas between F1 channel elements and salt-walls; composed of coarse-grained, horizontally-laminated, massive, climbing ripple-laminated, trough cross-bedded sand; represent partially confined flow events.



Minor gravel chute element
F8
 Small scale chute; originate from the convergence of non-confined flows in overbank settings; generally shallow (<0.3 m deep) and narrow (<20 m wide); typically filled with massive sets of medium-grained sandstone to granulestone (Fm) or crudely developed cross-bedding (ha Fxp/Fxt).

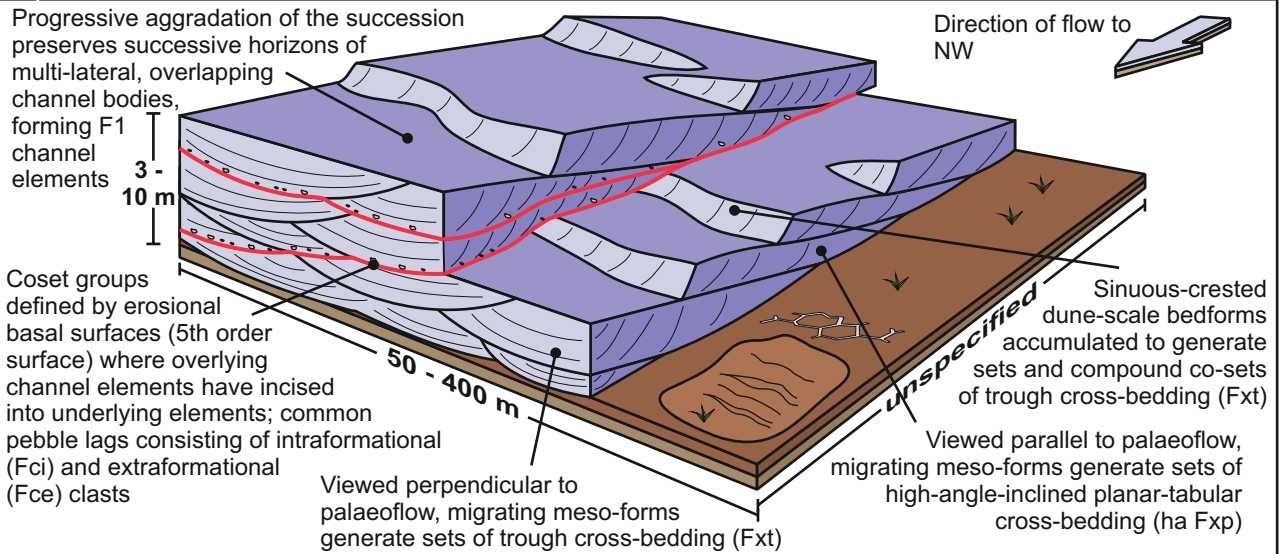


Pond element
F9
 Sheet-like body containing symmetric wave-ripple strata, overlain by thin siltstones; formed in response to wind blowing across bodies of standing water in floodplain areas; siltstones overlying wave-ripple strata represent the accumulation of loess.

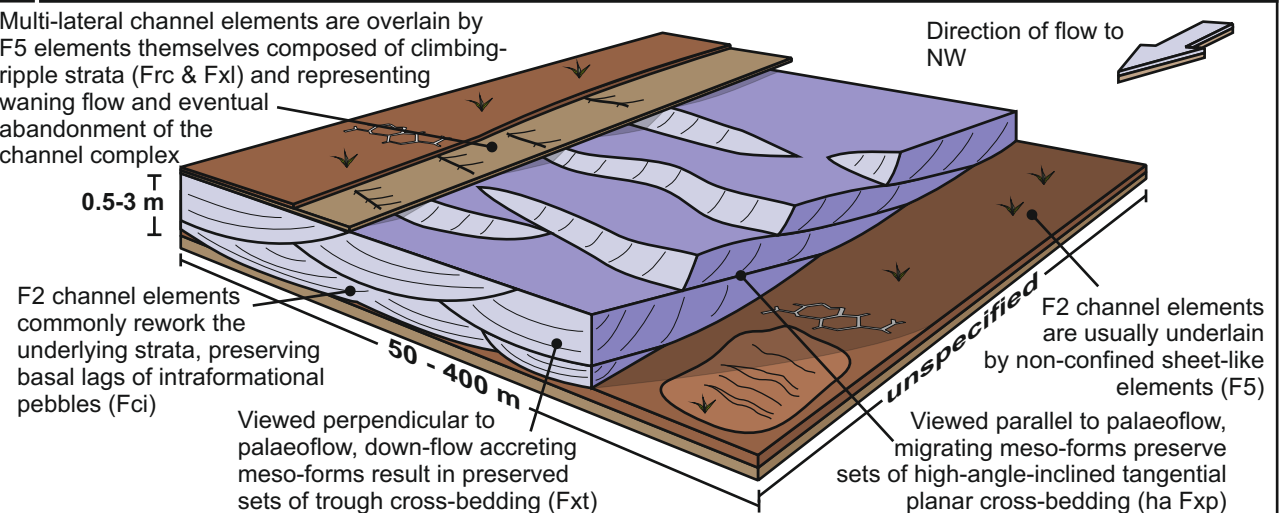
Fluvial Channelised

Fluvial non-channelised (overbank)

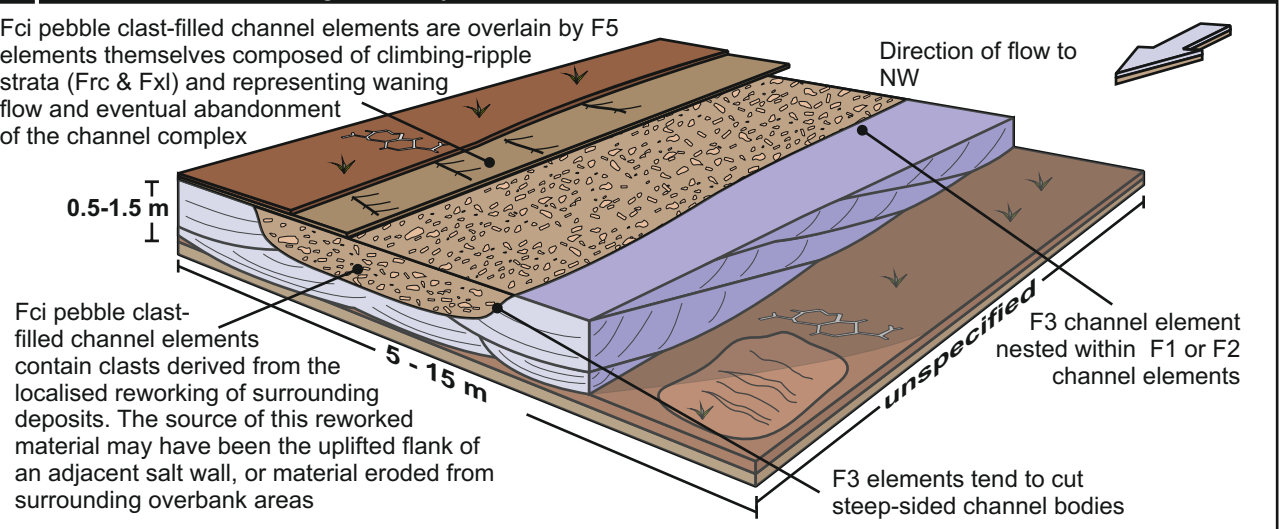
a Element F1: Multi-storey, multi-lateral channel elements

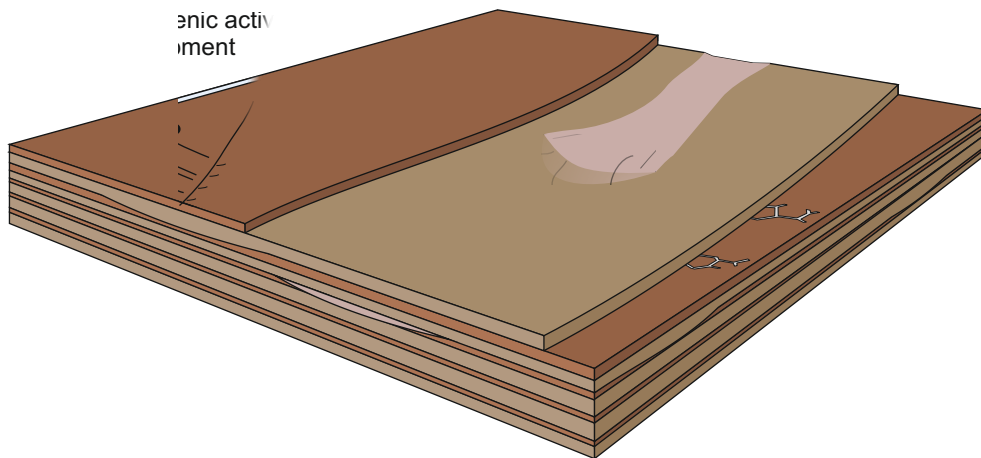


b Element F2: Single-storey, multi-lateral channel elements



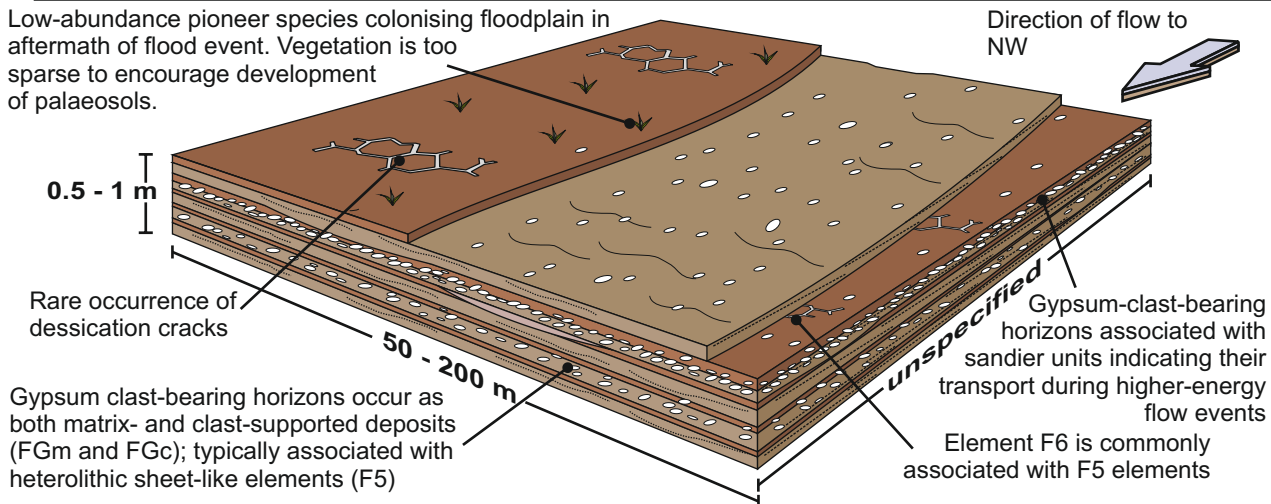
c Element F3: Single-storey, unilateral intraformational-clast fill channel element





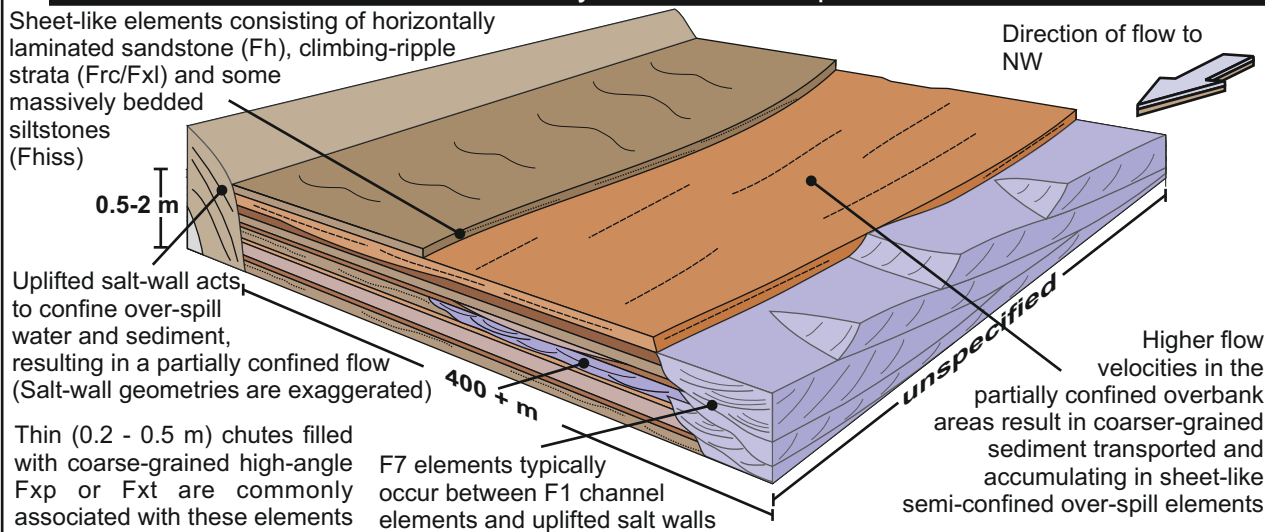
Element F6: Non-confined heterolithic sheet-like deposits with gypsum clast horizons

Low-abundance pioneer species colonising floodplain in aftermath of flood event. Vegetation is too sparse to encourage development of palaeosols.

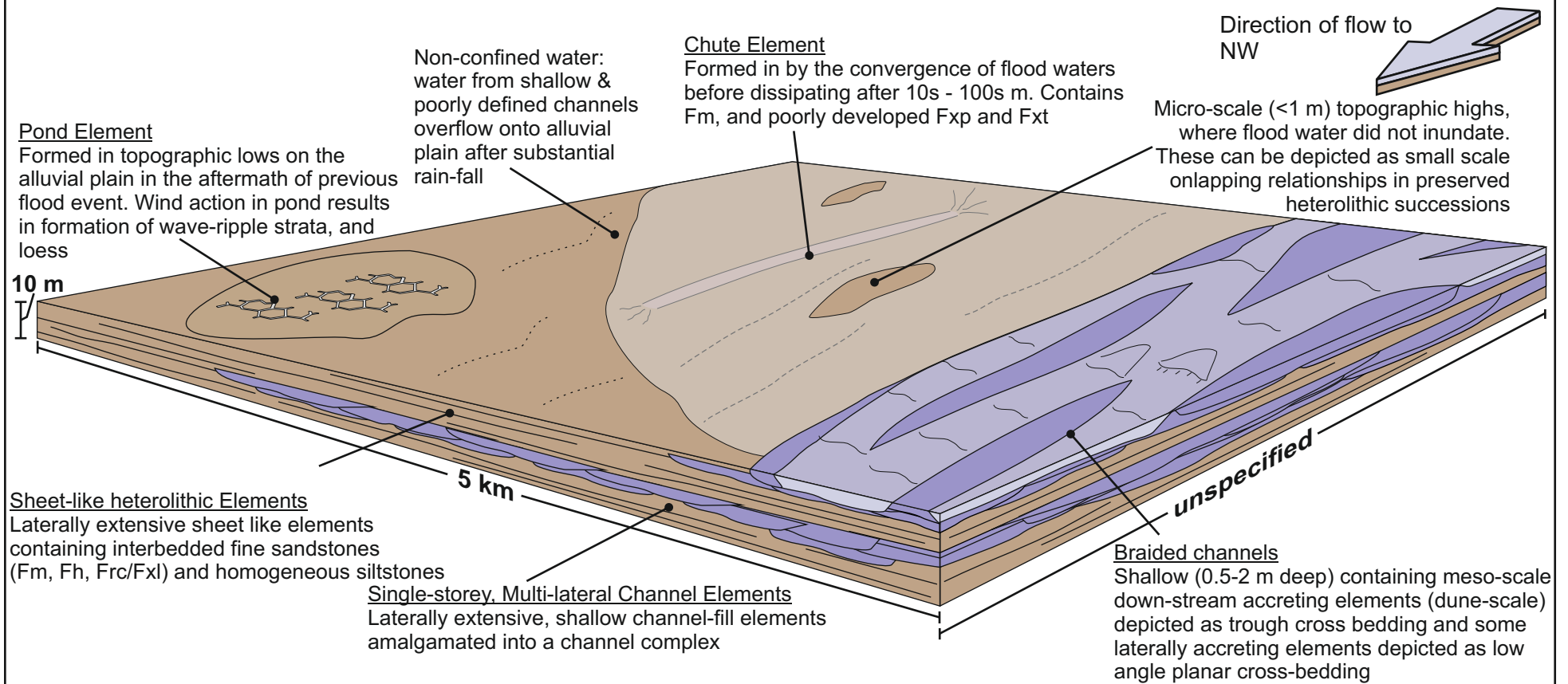


Element F7: Partially-confined over-spill elements

Sheet-like elements consisting of horizontally laminated sandstone (Fh), climbing-ripple strata (Frc/Fxl) and some massively bedded siltstones (Fhiss)

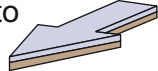


General Depositional Model: Channelised & Non-Channelised Elements



Depositional Model: Fisher Basin & Parriott Basin deposition style

Direction of flow to
NW



Sand-prone mini-basin (Fisher Basin)

Sand-prone basin is characterised by high ratio of sand to argillaceous material. These basins tend to have high proportions of channelised, and associated elements

Single-storey, Multi-lateral Channel Elements

Laterally extensive, shallow channel-fill elements amalgamated into a "channel sheet". These elements are generally isolated within heterolithic sheet-like elements

Multi-Storey Multi-Lateral Channel Elements (F1)

Laterally amalgamated channel elements become vertically amalgamated as the fluvial system aggrades

Fisher basin

Parriott basin

Fisher Valley salt wall

Partially-confined over-spill elements

Form between channelised elements and salt walls which act to partially confine water, increasing water velocity, allowing larger grained material to be transported

Heterolithic Sheet-like Elements

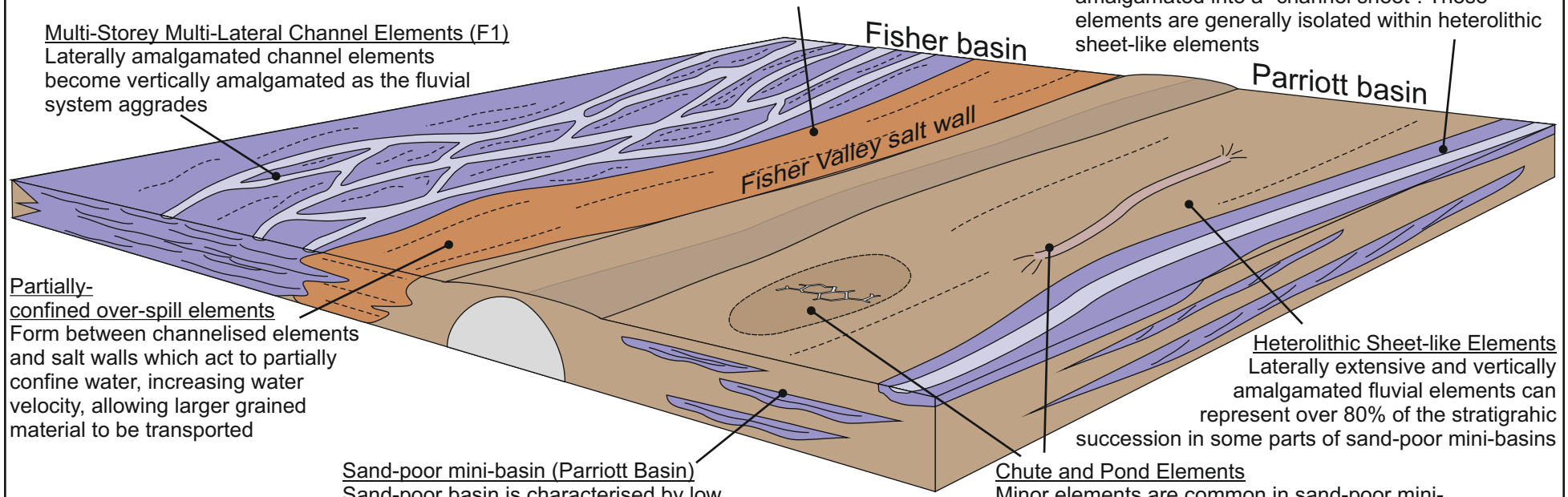
Laterally extensive and vertically amalgamated fluvial elements can represent over 80% of the stratigraphic succession in some parts of sand-poor mini-basins

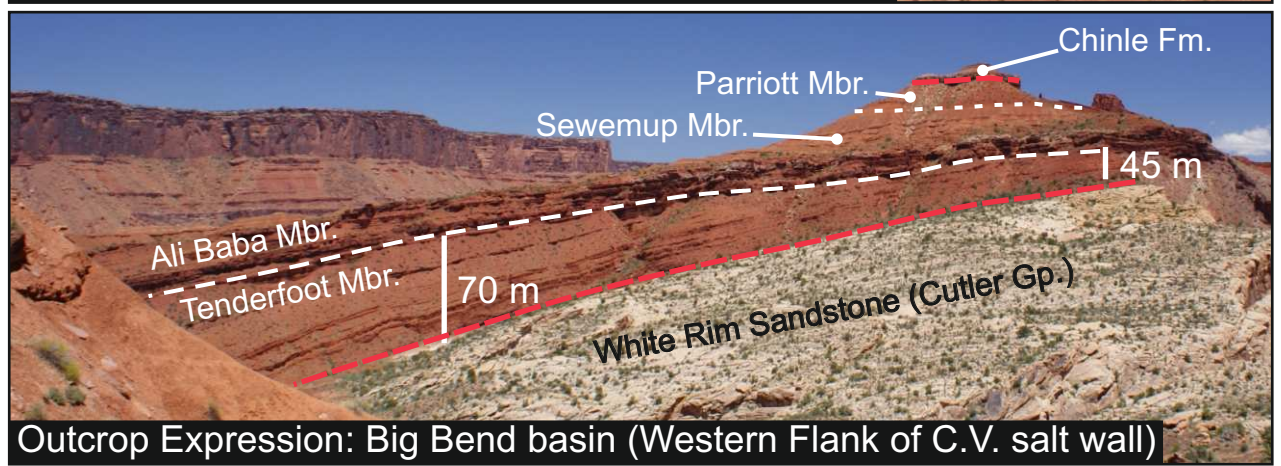
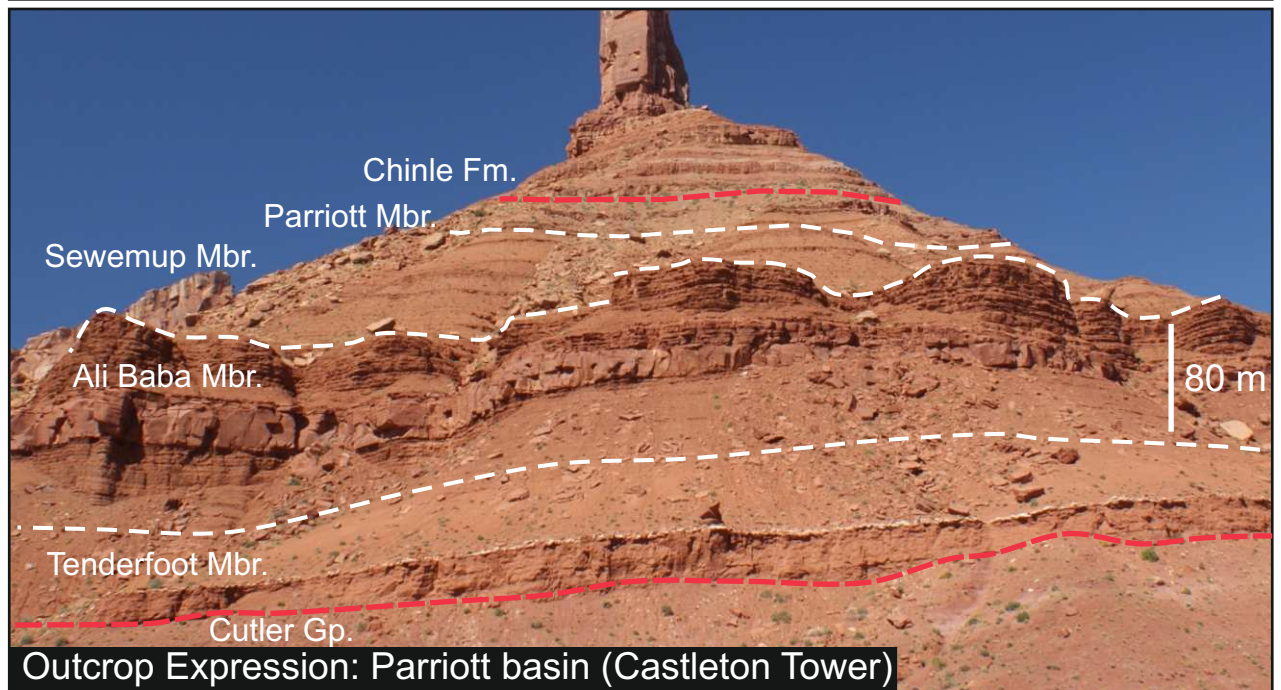
Sand-poor mini-basin (Parriott Basin)

Sand-poor basin is characterised by low ratio of sand to argillaceous material. The fill of these basins tend to be filled with non-confined elements and associated elements

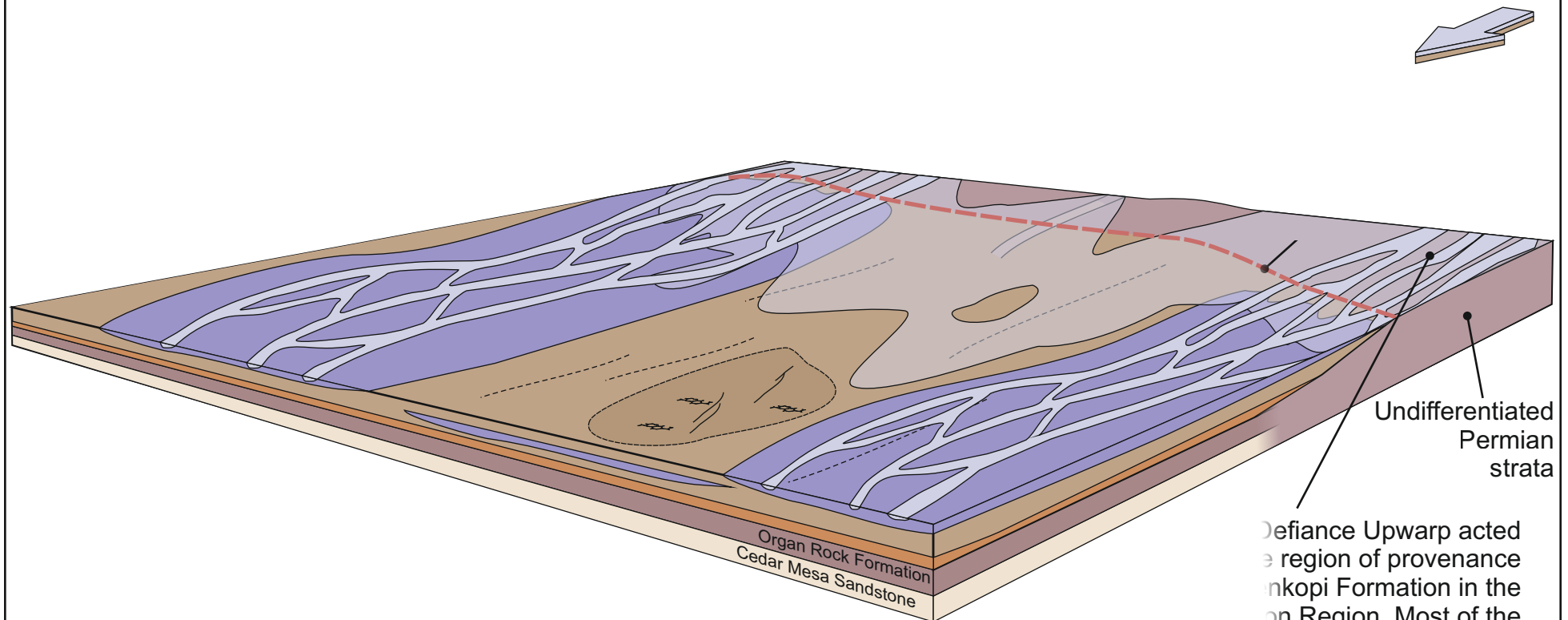
Chute and Pond Elements

Minor elements are common in sand-poor mini-basins, representing convergence and dissipation of non-confined flood waters, and the pooling of flood water in the aftermath of flood events

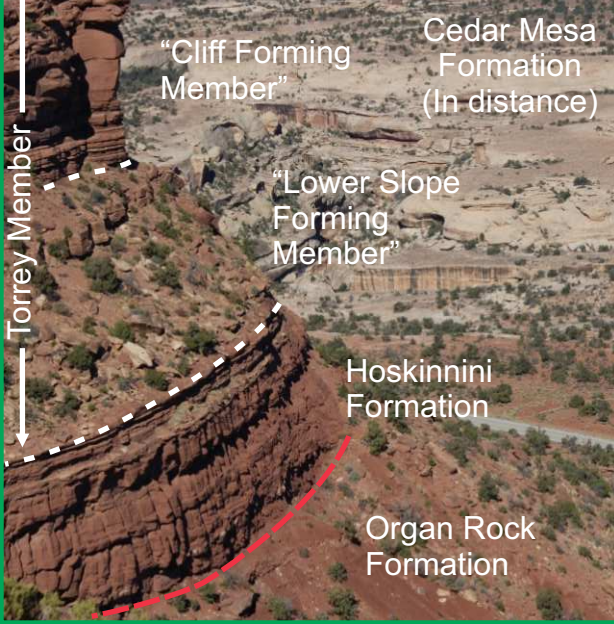




Regional Depositional Model: White Canyon Region



Typical outcrop expression



Gypsum Horizon, Hoskinnini Mbr



"Wavy" Beds in Hoskinnini Mbr.



Regional Depositional Model: Salt Anticline Region & White Canyon Region

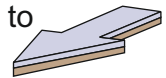
Salt Anticline Region

Multiple sediment supply areas: Uncompahgre and San Luis uplifts. Salt walls control distribution of sediment in the evolving mini-basins, resulting in contrasting stratigraphic successions developing in adjacent mini-basins. Thickness of Moenkopi Fm is extremely variable due to differential rates of subsidence within the various mini-basins

Uncompahgre & San Luis Uplift

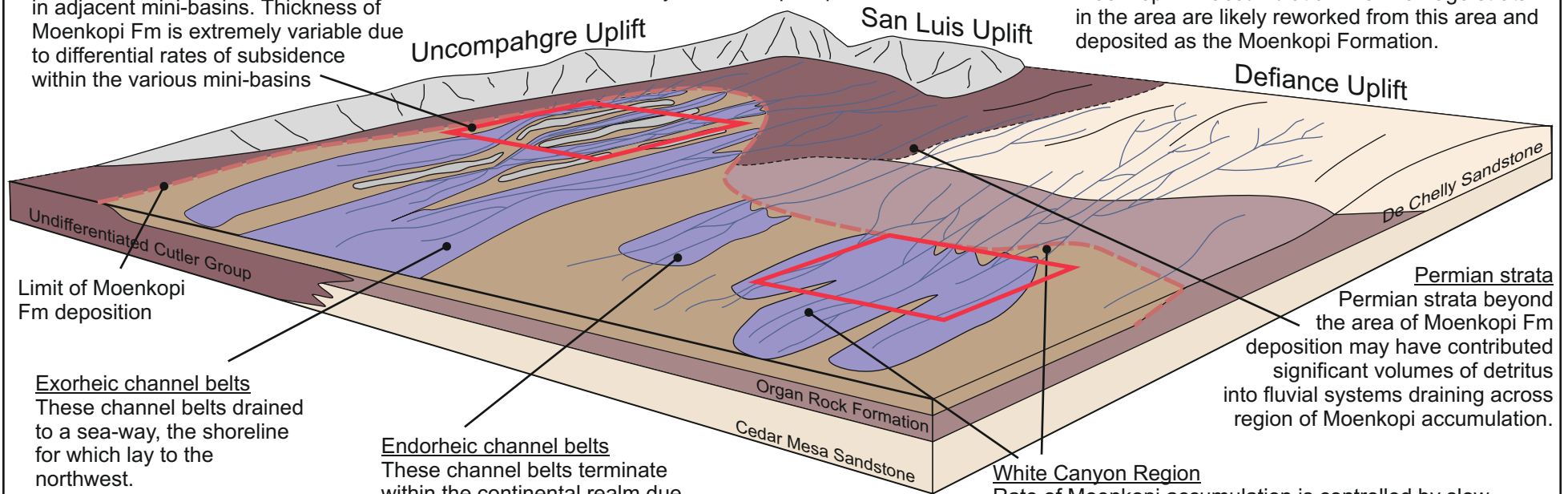
These two uplifted areas are composed of crystalline basement rock, and persisted as significant topographic features until late in the history of Moenkopi deposition.

Direction of Flow to NW



Defiance Upwarp

An upland area throughout the history of Moenkopi Fm accumulation. Permian age strata in the area are likely reworked from this area and deposited as the Moenkopi Formation.



Limit of Moenkopi Fm deposition

Exorheic channel belts

These channel belts drained to a sea-way, the shoreline for which lay to the northwest.

Endorheic channel belts

These channel belts terminate within the continental realm due to transmission losses before the fluvial system reaches the sea-way.

White Canyon Region

Rate of Moenkopi accumulation is controlled by slow tectonic subsidence, resulting in a relatively thin succession accumulating over broad area. Sediment accumulating in this region are mainly derived from the Defiance Upwarp.

Permian strata
Permian strata beyond the area of Moenkopi Fm deposition may have contributed significant volumes of detritus into fluvial systems draining across region of Moenkopi accumulation.